A PLETHYSMOGRAPHIC DEVICE FOR DETERMINING HUMAN BODY VOLUME AND BODY DENSITY

Thomas Frederick Cronjé

A dissertation submitted to
the Faculty of Medicine at the University of Cape Town
in partial fulfilment of the requirements for
the degree of Master of Science in Medicine
in the field of Biomedical Engineering.

September 1992

ACKNOWLEDGEMENTS

I would like to thank the following people for their contributions to this project:

Professor A.E.Bunn, for serving as supervisor of the project, for his guidance and for spending many hours proof-reading this thesis.
My wife, for supporting me, and for her endless encouragement and patience throughout the course of the project.
The staff of the electronic workshop of this department for generously sharing their technical knowledge and always being available to help.
The staff at the mechanical workshop of this department for constructing various components for the project.
The staff and students of this department for their encouragement.
Certain staff members of the Wynberg Military Hospital, the Groote Schuur Hospital, and the Red Cross Childrens' Hospital for offering their facilities, and for performing tests on subjects (namely body composition and lung function testing).
The subjects, for enduring the regime of, at times, uncomfortable tests.
My father, for his advice, theoretical and technical help, his interest and encouragement.
My mother, family and friends for their encouragement and support.

Finally I wish to thank the South African Medical Research Council for their financial assistance.

THE BODYBOX

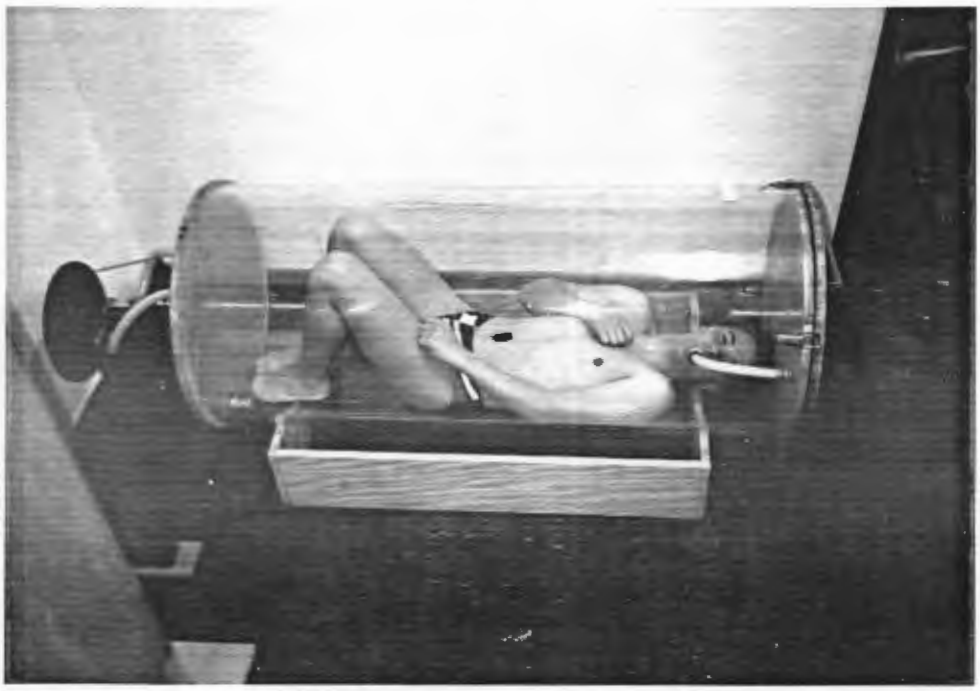

ABSTRACT

The measurement of total body volume (V) (excluding lung volume) together with total body mass (m) is required in order to determine body density (d = m/V). From this, and using certain simplifying assumptions, it is possible to derive body composition in terms of fat mass (FM) and fat free mass (FFM) for the two compartment model.

The standard method for determining body volume (and hence body composition) is the densitometric (underwater weighing) technique based on Archimedes' principle. Three variables, notably residual lung volume (RV), total body mass (m) and submerged body mass are measured. RV is normally determined using a gas dilution technique while total body mass is simply measured using an accurate weighing scale. The submerged body mass is measured while the subject is totally submerged in a tank of water. This method, although relatively accurate, requires substantial apparatus and is time consuming.

An alternative method, based on a polytropic thermodynamic process, is described for body volume measurement and thereby for body composition assessment. Previous use of this method by Taylor, et al. (1985) and Gundlach and Visscher (1986) were successful, but complex in terms of operating system.

The described system comprises of a perspex, sealed chamber. A cycling piston communicates with the chamber and imposes a minute sinusoidal pressure variation which is then measured. With a subject situated inside the chamber an increased pressure variation, caused by the decreased chamber volume, is then measured and processed to yield the displaced, or body volume. Subject comfort, above all, is greatly enhanced, in comparison to the underwater weighing method. A substantial advantage of the method appears to be that RV need no longer be measured.

Variables such as a rise of temperature and humidity caused by

the subject, as well as pressure variations due to respiration, were expected and found. These were analyzed both theoretically and experimentally and where necessary the data were modified to account for these variables using a personal computer. Calibration and preliminary validation of the instrument has been carried out using underwater weighing, bioimpedance and skinfold analyses and the error of measurement assessed.

It appears that the described plethysmographic method is capable of measuring body volume and thus compares favourably to the underwater weighing method. Even though other groups have succeeded in employing similar principles, a substantially simpler mechanism has been used here.

DECLARATION

I, THOMAS PATRICK CRONIN, hereby declare that the work on which this thesis is based is original (except where acknowledgements indicate otherwise), and that neither the whole or any part of it has been, or is to be submitted for another degree in this or any other University.

I empower the University to reproduce for the purposes of research only, either the whole or any portion of the contents.

Signed Signed by candidate

Date _____

Signature removed

TABLE OF CONTENTS

LIST OF FIGURES

LIST OF TABLES

1. INTRODUCTION

Body composition assessment has become an effective tool for determining nutritional or health status in man, and a popular method for assisting in fitness and performance monitoring of athletes and the health conscious population at large. Overfatness (obesity) has numerous problems associated with it, namely high blood pressure and arteriosclerosis, a higher incidence of circulatory, breathing and kidney problems, diabetes, bone and joint degeneration, a higher risk of respiratory infections, as well as psychological maladjustment.

Most methods for assessing body composition are based upon the two compartment model in which the body consists of two distinct components, fat mass (FM) and fat free mass (FFM). Fat, a stored triglyceride, is almost anhydrous, and has a density of about 0.9 g/cc at 37 ^{0}C, while the fat free body has a density of about 1.1 g/cc at the same temperature (Keys and Brozek, 1953). On the assumption that the fat free body and the fat are separable, homogeneous masses, this significant difference between the densities permits the calculation of the relative amounts, FM and FFM, provided the whole body density is known.

Net body volume (v) and body mass (m) are required when determining body density in man (d = m/v). Body density, in turn, can be substituted into the formulae of either Siri (1961) or Brozek, et al. (1963) to yield body composition in terms of FFM and FM which combined yields total body mass (m).

$$SIRI : \%\ BODY\ FAT = 100\left(\frac{4.950}{DENSITY} - 4.500\right)$$

$$BROZEK : \%\ BODY\ FAT = 100\left(\frac{4.570}{DENSITY} - 4.142\right)$$

where DENSITY is the body density in g/cc. However, the formulae above are controversial as they are based on density assumptions which are unlikely to be valid in all subjects. These should consequently be used with caution. In this dissertation percent body fat is nonetheless calculated using the equation of Siri

with the realisation that the results obtained should be treated with circumspection.

The most accepted and common method for determining body volume is the underwater weighing method. Underwater weighing utilizes Archimedes' principle and involves a number of measurements including:

- total body mass (m);
- underwater body mass (the subject is submerged);
- residual lung volume (RV);
- water temperature;

An estimate of intestinal gas volume is also needed for an accurate determination of body volume.

Difficulties and disadvantages inherent in this method include:

- subject acceptance and cooperation;
- necessity for subjects to do pre-test runs in order for them to familiarize with the procedure and to produce consistent values;
- relatively time consuming (usually greater than 30 minutes);
- ill patients, children and the frail cannot be expected to submerge themselves in water.

Accuracy in terms of repeatability or reproducibility (Liedtke, 1986) is mainly based on :

- the ability of the operator to read a fluctuating scale pointer;
- the ability of a subject to completely exhale to RV when submerged;
- measurement of the subject's intestinal gas volume which is virtually impossible and which is in a continuous state of flux.

1.1. Aim of thesis

The aim of this thesis is to design and construct a plethysmographic (plethysmography is the measurement of change

in volume) device for determining total body volume based on a polytropic thermodynamic process, bearing the above-mentioned problems in mind.

It is envisaged that the instrument should be :

* accurate and reproducible : comparable to the underwater weighing method;
* generally applicable : adults, children, as well as paraplegics and the frail must be measurable;
* acceptable to the subject : non-invasive, comfortable and quick;
* easy to operate and service : no skilled staff required;
* affordable.

1.2. Thesis structure

The thesis is divided into five functional parts, the background, which includes a review of the relevant literature and a description of the principle and relevant theory, the design and construction, which includes the hardware and software, the acoustic modelling and analysis, the functional evaluation of the system, which includes the examination of influencing factors, the calibration, the verification of the lung exclusion and a preliminary validation of the system (tests on subjects), and the conclusions and recommendations for further research and development.

2. LITERATURE REVIEW

2.1. Introduction

Biologists and physiologists have always been curious about mammalian (and in particular human) body composition, in terms of its gross biochemical constituents like protein, fat, water and mineral. Consequently a great number of studies on body composition have been conducted, with the primary goal of acquiring accurate representative data for different groups in health and disease. These factors have provided the stimulus for the evolution and development of numerous techniques for the measurement or assessment of body composition.

Research on indirect techniques for human body composition studies was pioneered by Behnke (1942). He and his associates used the densitometric underwater weighing technique based on Archimedes' principle and they developed a formula for calculating the composition, in terms of fat mass and fat free mass. A detailed analysis of this technique by Keys and Brozek (1953) appeared a decade later. To date this technique has enjoyed the status of the "accepted method" or the "gold standard" for body composition assessment, due to its fundamentality, non-invasiveness and reasonable accuracy.

2.2. Other body composition methods

Apart from densitometric methods there are electromagnetic (e.g. perturbation of an electromagnetic field by the body electrolytes (EMME)), biochemical (e.g. urine analysis, isotope dilution), radiation (e.g. X-rays, computed tomography, neutron activation analysis, dual photon absorptiometry, infrared interactance, ultrasound), anthropometric (e.g. skinfolds, bone dimensions, limb diameters), metabolic or chemical (e.g. energy balance and nitrogen balance) and electroconductive methods (e.g. bioimpedance analysis (BIA) and total body electrical conductivity (TOBEC)). The BIA method currently enjoys a lot of

attention due to its ease of use and comparative accuracy while skinfold analysis probably remains the most common method of use due to cost.

Other methods include photogrammetry by Pierson (1963), a decompression method by Kodama and Pace (1963), helium displacement by Fomon, Jensen and Owen (1963).

2.3. Body volumetry

The following review is based on those methods aimed at measuring body volume and hence density in the determination of body composition. Body density is the quotient of body mass and (gas free) body volume. Accurate measures of body mass can be obtained simply by using a standard calibrated weighing scale. The measurement of total body volume poses more difficulties and methods to measure body volume have therefore grown in number. Apart from underwater weighing there is the water displacement method (Garn and Nolan, 1963). These two methods compare favourably and are considered reliable (Ward, et al., 1978). However, they both require total immersion in water and are therefore not feasible for use on infants, paraplegics, or the frail. A combination of water and air displacement has been used by Garrow, et al. (1979). This method proved more convenient and was advocated by Buskirk and Mendez (1984) for sport science applications, yet it remains cumbersome and incompatible with paraplegics and the frail.

The standard densitometric method, namely underwater weighing, requires an accurate residual lung volume measurement during submersion and an intestinal gas volume correction, the latter of which may be inaccurate by up to 300 ml (Buskirk, 1961). This method involves a cumbersome procedure for the researcher or operator, as well as an uncomfortable, fairly time-consuming procedure for the subject.

Another volumetric method, acoustic plethysmography, has been

used by Deskins, et al. (1985) and Sheng, et al. (1988). This method employs the Helmholz resonance principle whereby a cavity resonates at a frequency proportional to the inverse square root of the cavity volume. By placing a body inside the cavity and by applying a swept frequency of acoustic waves the resonance can be analyzed to yield the remaining cavity volume. These groups developed devices, which estimate premature infant volumes, with resonance frequencies around 100 to 120 Hz. This method is not suitable for estimating adult volumes since the required operating frequencies will be subsonic (below 20 Hz) and hence difficult to generate and detect, if commercial loudspeakers and microphones are to be used.

More recently, Taylor et al. (1985) and Gundlach and Visscher (1986), managed to overcome the problems inherent in the underwater weighing method by developing devices, based on Boyle's law, which measure total body volume. The subject is placed in a sealed vessel to which a plunger is connected. Past attempts at perfecting such a method were unsuccessful due to the rise of temperature and humidity caused by the subject, heat production during the compression phase of the plunger stroke and pressure fluctuations caused by respiration.

These two plethysmographic methods were validated against the underwater weighing method showing virtually insignificant differences and excellent correlations. Subject comfort was considerably enhanced. The majority of air-filled spaces within a subject's body, ie. lungs and intestinal gas, were found not to contribute to the apparent body volume (Gundlach and Visscher, 1986). Net body volume is the result.

Both devices employ a second reference chamber with its own independent piston mechanically coupled to the measuring chamber's piston. The device of Gundlach and Visscher (1986) is housed in a temperature controlled room, uses heat exchange coils (with a thermostatic bath) around the pipes connecting the pistons with the chambers and uses metabolic heat extracting bags

to envelope the subject. For each subject to be measured the device is calibrated with a set of known volumes.

Taylor, et al. (1985) utilized a novel technique by developing a dynamic system. Sinusoidally moving pistons cause sinusoidally varying pressures in the chambers which are measured in relation to each other and harmonically analyzed to yield the body volume. Surface area effects were studied and corrected (instead of using heat extracting bags described above).

The drawback of these plethysmographic devices is that they both appear to be complex in terms of operation and mechanism.

2.4. Conclusion

The goal of this study is, therefore, to devise a "BODYBOX" which is mechanically simpler than those devised by Taylor, et al. (1985) and Gundlach and Visscher (1986), and which has all corrections (i.e. pressure leaks, heat effects and general calibration) and the final analysis (in terms of body volume and density) automatically performed by a personal computer.

3. THE PLETHYSMOGRAPHIC CONCEPT AND THEORETICAL CONSIDERATIONS

3.1. Introduction

In the first part of this chapter the concept of plethysmographic measuring is explained and illustrated. In the second part the pressure-volume theory employed in the development of the plethysmographic system is discussed. A displaced volume expression is derived and presented in a simplified form. Concepts like heat, leaks and humidity are also discussed.

3.2. The plethysmographic concept

In a system (entirely enclosed or sealed and within rigid walls) the behaviour of a gas can be expressed as pV^k = constant, where p is the pressure, V the volume and k the polytropic exponent. k is also known as the specific heat ratio and is expressed as the specific heat of a gas at constant pressure divided by the specific heat of the gas at constant volume (c_p/c_v). k is constant at temperature changes in the order of 10 ^{0}C and is dependent on the nature of the process. The entire range for k lies between one for an isothermal process and 1.67 (monatomic gasses) for an adiabatic process. For air (diatomic gas mixture) the practical limits are 1.0 - 1.4 for the isothermal to the adiabatic case.

Consider the general case where the system is a rigid, sealed chamber in which air is contained. Figure 3.1 (a) depicts such a system. Figure 3.1 (b) shows the same system with its volume content reduced by ΔV, causing an increase in pressure of Δp. Figure 3.1 (c) depicts a further development of the foregoing figures where a subject or body, now situated in the chamber, displaces a volume of air equal to its own volume. A relationship arises which now includes body volume as one of the variables. Hence the body volume can be calculated, provided the other variables are known or measured.

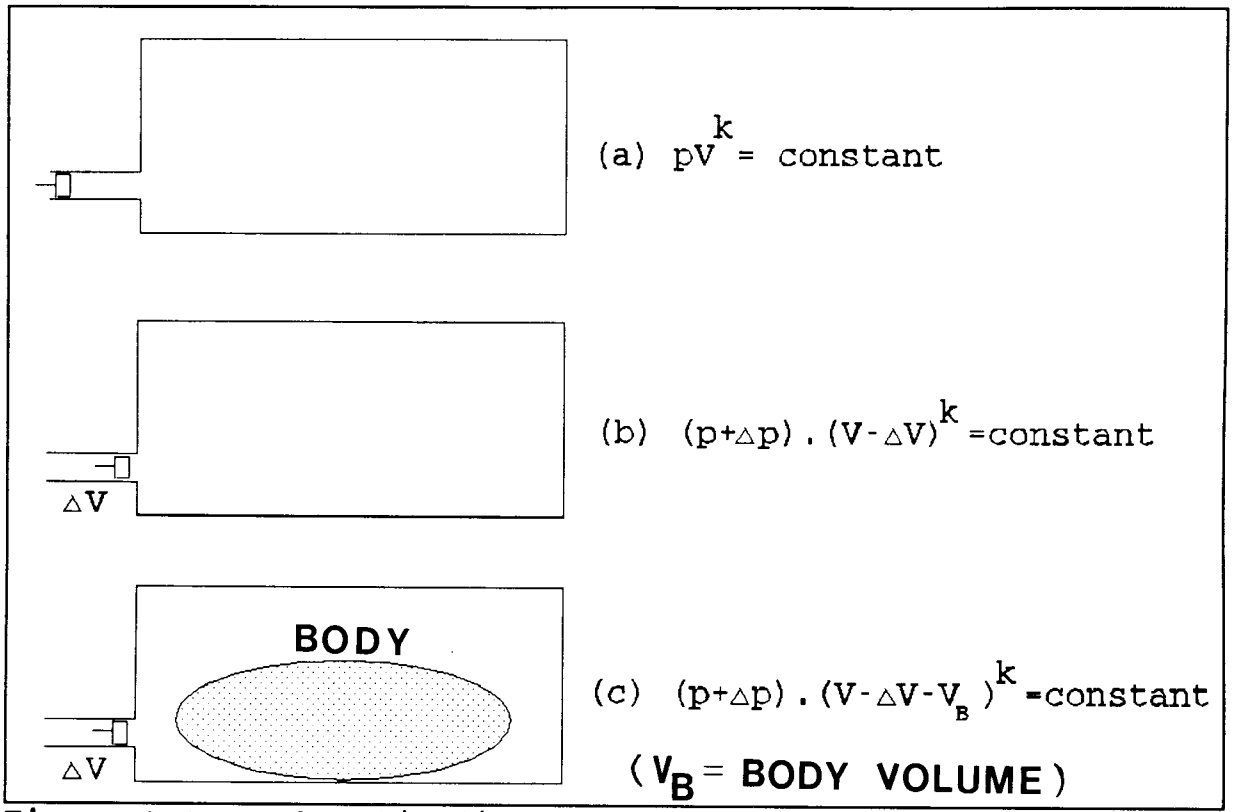

Figure 3.1 : Schematic diagrams of:
(a) a rigid, sealed chamber;
(b) the chamber, with a volume reduction of ΔV;
(c) the chamber, with a body.

The lung volume and intestinal gas, which may be in communication with the chamber's contained air, will be excluded from the apparent body volume (Gundlach and Visscher, 1986). This is valid, or partially so, if there exists a compliant pathway, be it via tubes and/or compliant, soft tissues.

If the piston, used to reduce the volume, is cycled by a constant speed crank-mechanism it will exhibit a sinusoidal movement and a sinusoidal Δp will occur. If the speed of the sinusoid is sufficiently high, so that the period of a single sine wave is sufficiently short in relation to the heat dissipation time-constant of the chamber, then the process will exhibit an adiabatic behaviour. If the period of a wave is much larger, or of the order of the heat dissipation time-constant, the system will behave isothermally. Possible drops in pressure differences

(between inside and outside) due to pressure leaks may require shorter operating sine wave periods, rather than longer ones. Operating frequencies will be selected to ensure that an adiabatic process where k = 1.4 is most likely (for air the adiabatic gas constant k is often designated by γ).

3.3. Deriving the body volume expression

Consider the "empty" chamber in figure 3.1 with a volume of V_C. If this becomes occupied by a displacement volume of V_B and, with the chamber now sealed, the volume is further reduced by the piston stroke volume ΔV , it follows that:

$$P_C(V_C-V_B)^{k} = (P_C+\Delta p)(V_C-V_B-\Delta V)^{k} \qquad (1)$$

where Δp is the corresponding change in pressure and P_C (usually equal to atmospheric pressure P_A) is the pressure inside the chamber. Making V_B the subject of the expression, it is found that:

$$V_B = V_C - \frac{\Delta V}{1-(\frac{P_C}{P_C+\Delta p})^{1/k}} \qquad (2)$$

Rearranging equation (2) by simplifying the denominator of the second term, and substituting $-1/k$ with β gives:

$$V_B = V_C + \frac{P_C^{\beta}\Delta V}{(P_C+\Delta p)^{\beta}-P_C^{\beta}} \qquad (3)$$

The denominator of the second term can now be expanded using Taylor's series:

$$(P_C+\Delta P)^{\beta}-P_C^{\beta} = P_C^{\beta}+\beta P_C^{\beta-1}\Delta p+\frac{\beta(\beta-1)P_C^{\beta-2}\Delta p^2}{2!}+\ldots-P_C^{\beta} \qquad (4)$$

The right-hand side reduces to:

$$R.\,H. = \beta P_C^{\beta-1}\Delta p[1+\frac{(\beta-1)P_C^{-1}\Delta p}{2!}+\frac{(\beta-1)(\beta-2)P_C^{-2}\Delta p^2}{3!}+\ldots] \qquad (5)$$

Substituting for β, in terms of k, gives:

$$V_B = V_C - \frac{kP_C\Delta V}{\Delta p(1+R)} \qquad (6)$$

where R constitutes the remainder of a Taylor series, i.e.:

$$R = -\frac{(k+1)\Delta p}{2!kP_C} + \frac{(k+1)(2k+1)\Delta p^2}{3!k^2P_C^2} - \ldots \qquad (7)$$

The remainder is very much smaller ($\Delta p/P_C$: order of 1/1000) than unity, therefore *1/(1+R)* is virtually equal to *(1-R)*. Hence equation (6) becomes:

$$V_B \doteq V_C - \frac{kP_C\Delta V(1-R)}{\Delta p} \qquad (8)$$

and can be rewritten as:

$$V_B = V_C - \frac{kP_C\Delta V}{\Delta p} - V_{ERROR} \qquad (9)$$

where the error volume is:

$$V_{ERROR} \doteq -\frac{kP_C\Delta VR}{\Delta p} \qquad (10)$$

Since the second term of the remainder is very much smaller than the first term (as above : order of 1/1000), this can be neglected. The error volume is therefore:

$$V_{ERROR} \approx \frac{(k+1)\Delta V}{2} \qquad (11)$$

and equation (2) can be rewritten as:

$$V_B \approx V_C - \frac{kP_C\Delta V}{\Delta p} - \frac{(k+1)\Delta V}{2} \qquad (12)$$

Since $\Delta p << P_A$ which follows from the fact that $\Delta V << (V_C - V_B)$, the expected order of accuracy of equation (12) is in the region of 0.01 l (for a displacement of 70 l). This reduced expression will tend to have less error due to repetitive computational error, especially when considering the basic equation (2) where the second term calls for division by a very small entity.

3.4. Heat

Under equilibrium conditions the differential pressure between the inside and outside of the chamber will be zero. Metabolic heating of the inside of the chamber will cause an increase in chamber pressure P_C resulting in a baseline drift. From equation (2) it follows that:

$$\Delta p = P_C[(\frac{V_C - V_B}{V_C - V_B - \Delta V})^k - 1] \qquad (13)$$

The effect of this drift upon Δp will be proportional to the increase of P_C , and will be corrected accordingly.

3.5. Pressure leakage

A pressure leak of the chamber will also affect Δp. If a volume of gas is injected into the chamber (now with a leak) the rise in pressure will decay exponentially towards zero (with respect to atmospheric pressure). For a sinusoidal volume change, as obtained with a cycling piston, the leak will be proportional to the sinusoidal pressure change, Δp. By performing a volume calibration of the system or by knowing the leak time constant, this attenuation can be corrected.

3.6. Humidity

Different degrees of humidity may affect the accuracy of measurement. Increasing the water vapour content causes a marginal increase in air density. This could manifest itself as

a change in the specific heat ratio, k, and thereby introduce errors into the body volume determination.

As long as the air inside the system is unsaturated the air will behave in close accordance to an ideal gas, on which the employed pressure-volume theory is based. When saturation occurs, condensation of excess water may occur, whether in the form of fine droplets like mist and/or surface condensation. Condensation could lead to, on a microscopic basis, a large amount of heat being injected into the system, which in turn could cause errors in measurement. It is consequently advisable to avoid saturation.

3.7. Conclusion

Reliability will be improved by:

1. pre-warming of the system (at higher temperatures the system will be further away from saturation) or thermally controlling the environment;
2. excluding the subject's breath by having him/her breathe through a "snorkel" until shortly before the measurement period;
3. flushing the chamber between measurements with dry air;
4. including a canister of "damp-extracting crystals" (e.g. silica gel, slaked lime);
5. ensuring that the pressure leakage rate remains known;
6. waiting for the system to stabilize (in terms of the average chamber pressure), before measuring.

4. HARDWARE DESIGN

4.1. Introduction

This chapter describes the design of the hardware of the body volume measuring device (hereafter referred to as the BODYBOX). It is subdivided into two areas, namely the mechanics and the electronics. Figure 4.1 depicts the BODYBOX in terms of its gross components.

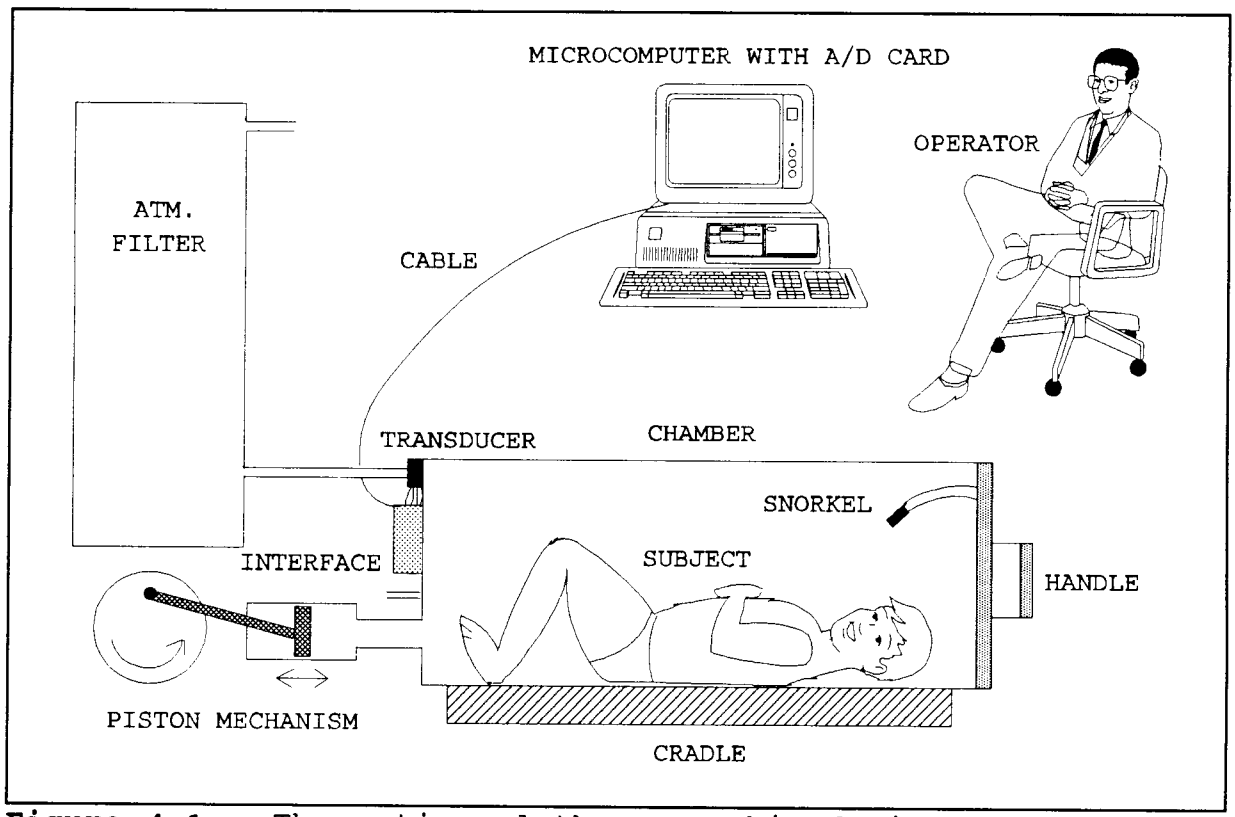

Figure 4.1 : The entire plethysmographic device (BODYBOX), in terms of its components.

4.2. Mechanics

4.2.1. Chamber

An airtight, rigid chamber with a door was constructed. It consists of a transparent, clear acrylic (perspex) cylinder of approximate dimensions of 1.5 m in length, 0.6 m in diameter and

a wall thickness of 14 mm (giving an internal volume of 390.2 l). The acrylic cylinder was donated to this department by the Groote Schuur Hospital. The ends were made up of a thick varnished pine block-board (thickness 20 mm). The fixed end was attached by screws and glued using a silicon sealant. The other end comprised of a lid which is removable and secured by heavy duty marine latches onto a thin, slightly compressible rubber gasket. Two wooden handles were attached onto the lid. The chamber was positioned horizontally to enable easy subject entry and exit. The entire chamber rests on a wooden cradle to isolate it from the floor as well as to stabilize it. A "snorkel" consisting of a flexible hose of length 0.3 m and inside diameter of 19 mm was connected to the inside of the lid via a hose flange. A disposable cardboard mouthpiece could be connected to the hose during the initial phase while a tapered rubber bung was used for sealing off the hose during the actual measurement phase.

A second chamber of approximately similar materials and dimensions was used for acoustic filtering in order to stabilize the environmental atmospheric fluctuations. This "acoustic filter" was simply attached to the other end of the differential pressure transducer via a short, semi-rigid tube and was itself open to atmosphere via a thin tube.

4.2.2. Piston mechanism

The piston mechanism (previously used as an artificial lung pump) consists of an electric AC motor geared down and coupled by a leather belt to an adjustable cam (for different stroke volumes). The cam drives a conrod, connected to a piston housed in a fixed bore cylinder. The piston oscillates sinusoidally at about 0.53 Hz (32 RPM) and generates a cyclical volume (stroke volume) with a maximum amplitude of 796 ml. This frequency is a compromise between a very low frequency on the one hand which is desirable due to pulmonary impedance which drops steadily with a drop in frequency, and a higher frequency on the other hand, which allows more rapid measurement. It is of note that the frequency band

of 6 to 10 Hz should be avoided due to pulmonary resonance in adult humans (Peslin and Fredberg, 1986) . A sinusoid is employed due to its mechanical simplicity, its freeness from harmonics and the suitability of complete linearity when filtering.

The piston communicates with the subject chamber via a flexible, circumferentially re-inforced tube of diameter 19 mm and length 0.4 m. The piston mechanism is thus not rigidly attached to the chamber so as to avoid mechano-acoustic vibrations.

4.3. Electronics

4.3.1. Physical sensors

The sensors required in the BODYBOX are two pressure transducers namely:
(a) a sensitive, linear differential pressure sensor which senses the pressure difference between the atmospheric pressure (P_A) and the chamber pressure (P_C). The operating limits are 0 - 3500 Pa (Honeywell 176PC14HD: for more details, consult appendix A);
(b) a linear absolute or atmospheric pressure sensor. The operating limits are 0 - 200 kPa (National Semiconductor LX0503A: consult appendix B, for more details).

4.3.2. Transducer interfaces

The differential (figure 4.2) and absolute (figure 4.3) pressure transducer circuits employ similar circuit design techniques (for the detailed circuit diagrams, see appendices C and D, respectively). In each circuit a precision voltage reference (LM10) is used to drive the resistive bridge arrangement of the sensor which in turn provides a voltage proportional to the applied pressure. This proportional voltage is then amplified by an instrumentation amplifier consisting of the standard symmetrical three-operational amplifier-configuration (LM324) which provides for suitable specifications of low noise, very

high linearity and stability, and high common-mode rejection. The differential pressure circuit employs a gain of the order of 500, the other a gain of 100.

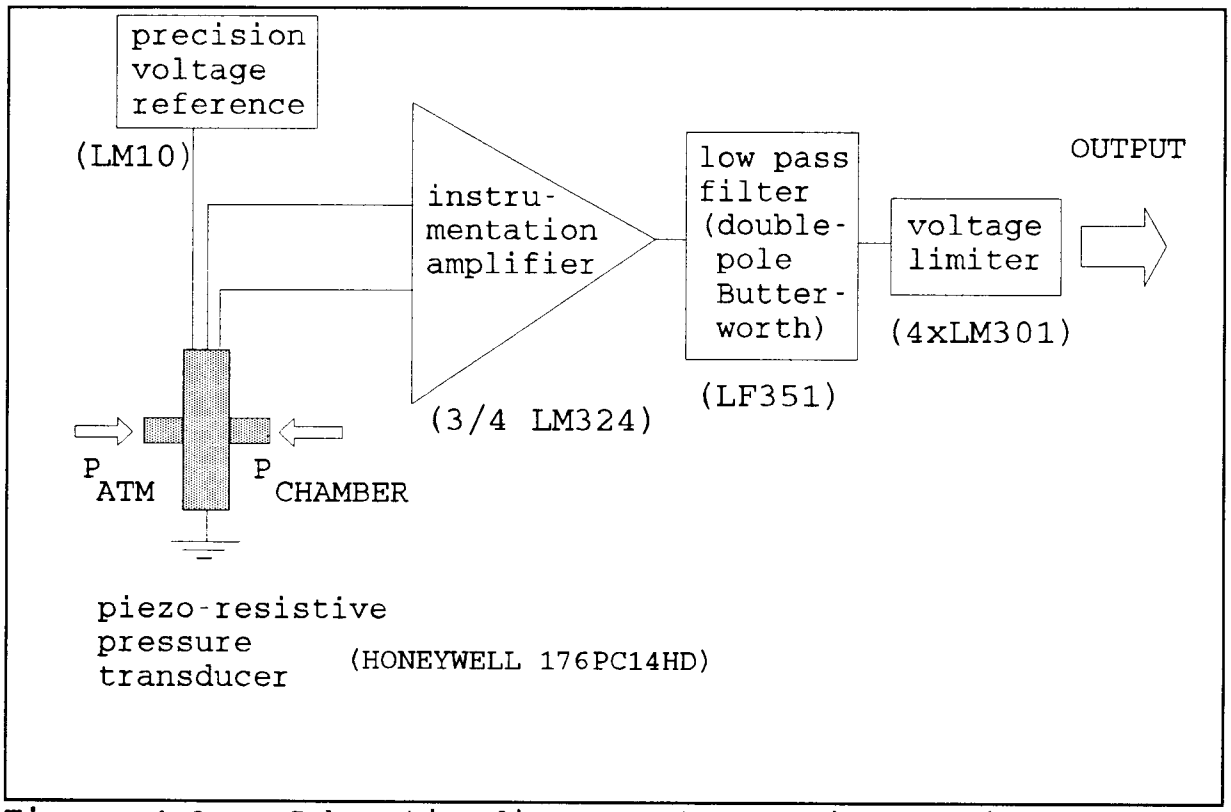

Figure 4.2 : Schematic diagram of the differential pressure transducer interface.

The output from the differential pressure circuit is fed into an active double-pole Butterworth low pass filter (LF444) with cut-off frequency of about 2 Hz. This filter serves as an anti-aliasing filter which is necessary to cut out the majority of the noise spectrum, which if converted to digital form contributes towards error. The final output of this circuit conforms to the format: $V_{OUT} = g(P_{CHAMBER} - P_{ATM})$, where V denotes voltage, P pressure, and g the overall system gain including the physical acoustic gain and the circuit gain. Finally, in order to protect the analogue to digital converter from voltages exceeding the range of -10 up to +10 Volts, a bipolar voltage limiter (LM301s) is employed.

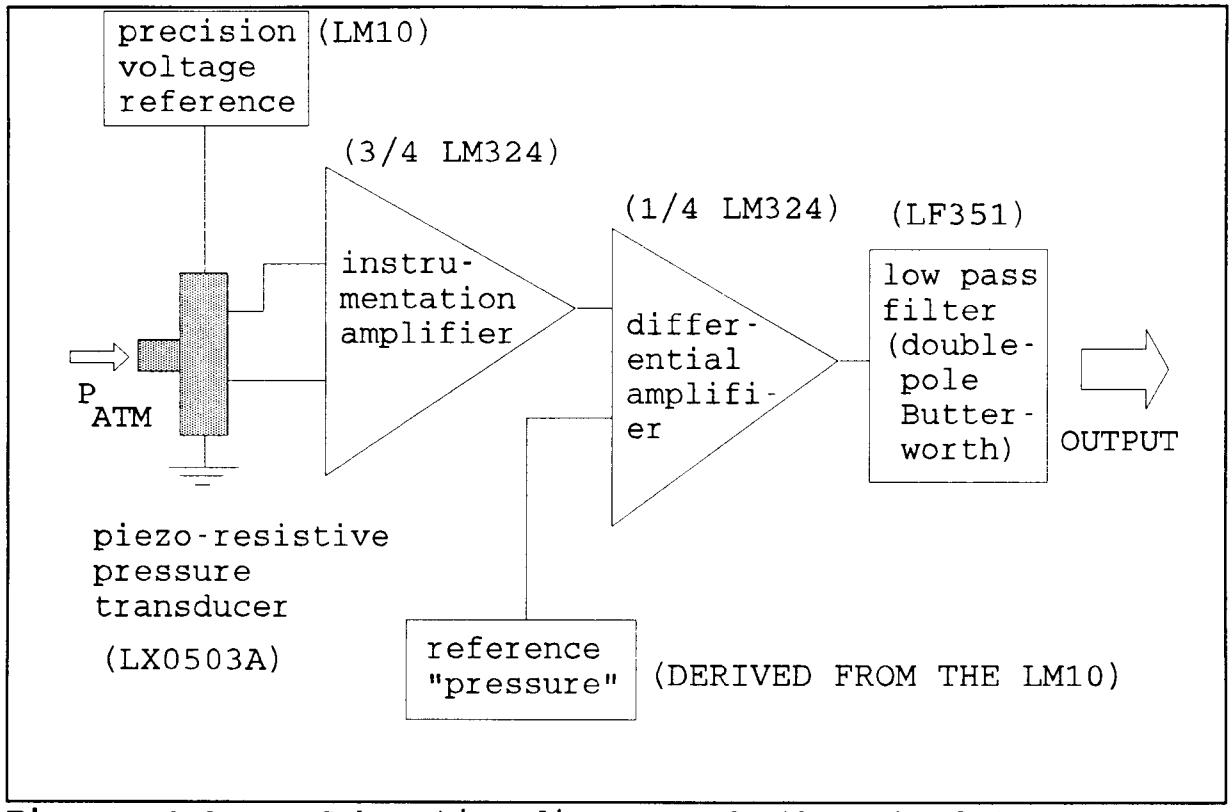

Figure 4.3 : Schematic diagram of the absolute pressure transducer (barometer) interface.

The output from the absolute pressure circuit is subtracted from, or compared to, a "reference pressure" which is realized by a presetable reference voltage. This difference is amplified by 10 to increase the sensor's sensitivity. A higher gain at this stage could be utilized only once sufficient circuit stability has been achieved. The output from the differential amplifier is then fed into a double-pole Butterworth low pass filter with similar characteristics as the above-mentioned filter, and for similar reasons. The final output of this circuit conforms to: $V_{OUT} = g(P_{REF} - P_{ATM})$, which is quite similar to the above transfer function.

4.3.3. Analogue to digital converter

The PC30 (from Eagle Electric Co. in Cape Town, South Africa) analogue to digital converter (ADC) was used. It is a 16 channel, 12-bit, 100 kHz, high input impedance, IBM-compatible,

plug-in ADC card. A sampling rate of approximately 100 per second was selected in order to provide sufficient accuracy while following the pressure sinusoid of 0.53 Hz. It is set for an input voltage range of -5 to +5 Volts.

4.3.4. Microcomputer

The microcomputer is based on an IBM-compatible PC/XT/AT. The minimum requirement is an IBM-compatible PC (personal computer) with a single floppy disc drive of 360 kByte and 560 kByte Random Access Memory with a Hercules monochrome video monitor.

5. SOFTWARE DESIGN

5.1. Introduction

The software forms a major part of the system development. Turbo Pascal version 6.0 was used to generate this software. A detailed description of the computer programme is given. This chapter is divided into the data capture and processing, and the keyboard/graphics interface. The former part discusses the sampling of data and the processing which consists of the pressure variation extracting algorithm. The latter part discusses the interface in terms of the menu and its elements.

5.2. Features

In order to make the programme as practical as possible it should be, amongst others,:

1. IBM-compatible;
2. user-friendly;
3. operative in real-time and be able to display waveforms during measurements;
4. menu-driven;
5. capable of file-handling (including saving, retrieving);
6. supportive of general screen graphics modes (e.g. Hercules).

5.3. Data capture and processing

The flow chart in figure 5.1 describes the programme called "BODYBOX" from a general perspective.

5.3.1. Initialization

The part of the developed software (which also utilizes the commercial software of the analogue to digital converter (ADC) card) which addresses the complete initialization of the total measuring system is discussed. In short initialization implies setting up the ADC, certain software parameters, and the entire

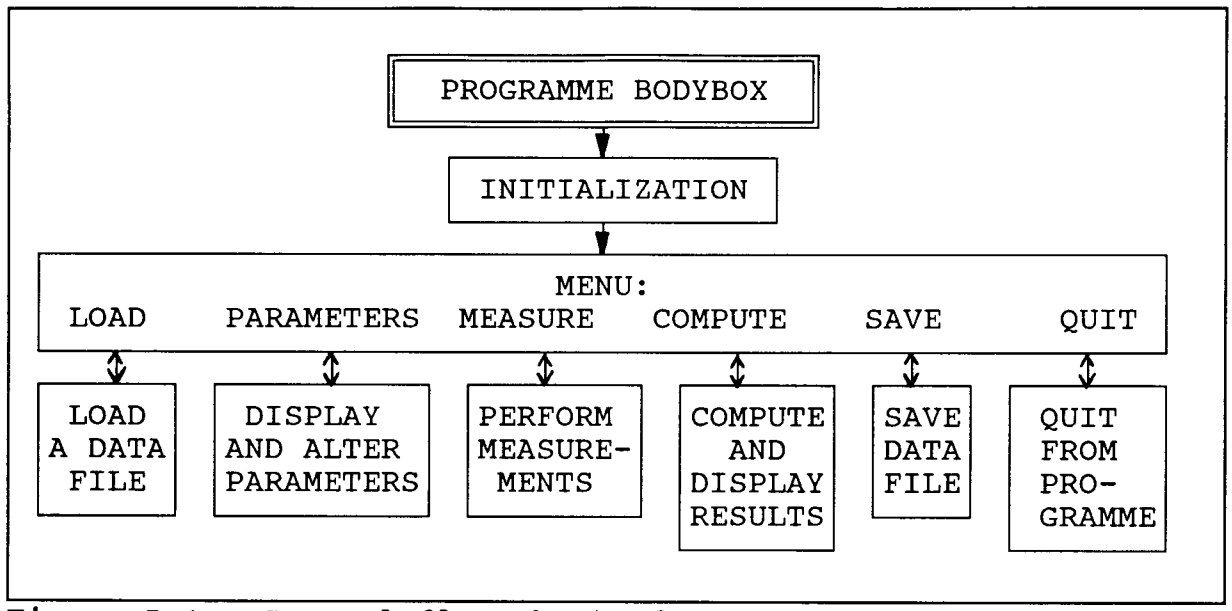

Figure 5.1 : General flow chart of PROGRAMME BODYBOX.

keyboard/graphics interface. This whole process is automatically performed once the software is started.

A sequential presentation of the initialization follows:

1. The PC30 (Eagle Electric, South Africa) ADC card is set up via the ADC's accompanying software by firstly calling up the diagnostics function (this checks whether the card is installed and is functioning correctly with any problems being reported on screen) and secondly by calling up the "init" procedure. If the card is not installed correctly or is faulty, the user is warned appropriately and is instructed to load files for analysis only, as opposed to carrying out measurements. In this case measuring is forthwith disabled.
2. The global arrays into which the sampled data (differential pressure and barometer pressure) are placed, are then initialized and cleared.
3. The screen graphics are initialized. A screen graphics unit (e.g. HERC.BGI) is required to be resident in the same directory or subdirectory in which the BODYBOX executable program file resides. If not the user is warned to this effect, and the program halts.

4. All default values (e.g. body mass, specific heat ratio (k)) are set.
5. The visual, menu-driven user-interface which concludes the initialization is displayed. It includes:

- a labelled pressure vs time (or voltage potential vs time) graph,
- a pressure "delta" (sinusoidal variations) analysis result window,
- a bias voltage window in which the hardware bias or offset voltage is displayed,
- an instruction window through which the user is always kept informed as to the present state of the programme and through which the user is often prompted to make decisions, and
- a constant display of the menu's command keys.

5.3.2. Sampling and information extraction

When an actual measurement is desired the user is required to engage the MEASURE function (see paragraph 5.4.2). Once in progress the system automatically samples the two transduced signals, namely the differential pressure (P_C - P_A) and the absolute pressure (P_A), and after sampling immediately automatically processes these sampled data values by applying an algorithm which extracts the appropriate data for further computation (see paragraph 5.4.3).

During sampling the resultant 12-bit data values (0 - 4095) are placed into their respective arrays namely the differential pressure array (DPA) and the absolute pressure array (APA). The data in the APA is averaged to yield a mean atmospheric pressure value. The data in the DPA represent the piston induced pressure variations, minus the atmospheric pressure. This array comprises of a sinusoidal pressure wave (in digital form) with an added rising (or falling) slope caused by metabolic heat from which the peak-to-peak values (which represent the pressure variations or "deltas" in the chamber) are extracted according to the following

algorithm:

1. Search for the first rising or falling edge of the wave. This is done by comparing the mean of the first two data points (samples) with that of the third and fourth data points. Comparing single samples may yield erroneous information if the signal is noisy. If the difference is less than a predetermined value (or zero), the next four samples are examined, and so on, until a reasonable difference is encountered. If the end of the DPA is reached without such a reasonable difference, "NO SIGNAL OR DC" is assumed and the user is informed. The reason for searching for an edge is three-fold, i.e. :

   - it establishes whether an appropriate signal exists;
   - it establishes where in the array or in time the wave starts, if for instance the piston had been started some time after the beginning of sampling;
   - it finds the position of the first slope or edge preparing the algorithm for further analysis.

2. From the first edge, find the following peaks and troughs and place these in an array. The first edge is tested for its slope. If the slope is positive the following sample is checked until the latter sample is no larger than the previous sample. The previous sample, a peak, is then placed into a peak array (PA). If the slope is negative, the same procedure is followed with the difference that the smallest next sample, a trough, is sought and placed in the PA. After a peak, or trough, is found, the next one is sought, and so on, until the end of the DPA is encountered.

3. Separate the peaks and troughs, which are at this stage interleaved in a single array, into their respective arrays. First a mean value is found of an even number of peaks and troughs. The values larger than the mean are placed, consecutively, into a peak array and the values smaller into a trough array. Range-limit values in the PA, for instance when the -5 or +5 Volt limits (values equal to 0 or 4095, respectively) are met, are replaced by zeros. This indicates clipping of the signal which is valueless for further analysis and further "peaks" and "troughs" are hence ignored.

4. From the peaks and troughs, calculate the consecutive geometric differences or "deltas" and place these values in an array. From figure 5.2 it is evident that a linear estimate is used each time to determine the imaginary in-between "peak" or "trough" from which the opposite, corresponding trough or peak is related. From this relationship a "delta" is generated. These "deltas" are consecutively placed into a delta array.
5. Discard "deltas" that vary more than 10% of the normal values. This serves as a rough filter. If such an "odd" value is encountered (e.g. when the subject accidentally breathes during measurement) the values of the next elements in the array are consecutively shifted back one position, in effect reducing the number of useful values by one. This is a minor handicap, since ten full pressure sinusoid waves are analyzed, which amount to twenty "deltas".

This concludes the algorithm and thus the processing. An error caused by the rising bias due to chamber heating has been analyzed (see appendix E) and shown to be of the order of 0.008 % (typical) to 0.032 % (worst case) of "delta" and is consequently neglected in the software analysis.

5.4. Keyboard/graphics interface

Each step of the general flow chart (figure 5.1) will now be discussed in detail. The "MENU" is broken down into its respective elements which are described below.

5.4.1. The menu

The MENU (see figure 5.1) is divided into its functions in the following order: measure, compute, load, parameters, save, and quit. It embodies a user-friendly interface which at all times keeps the user informed as to what is happening at the time and what the user is required to do next (e.g. start the piston mechanism, decide on options).

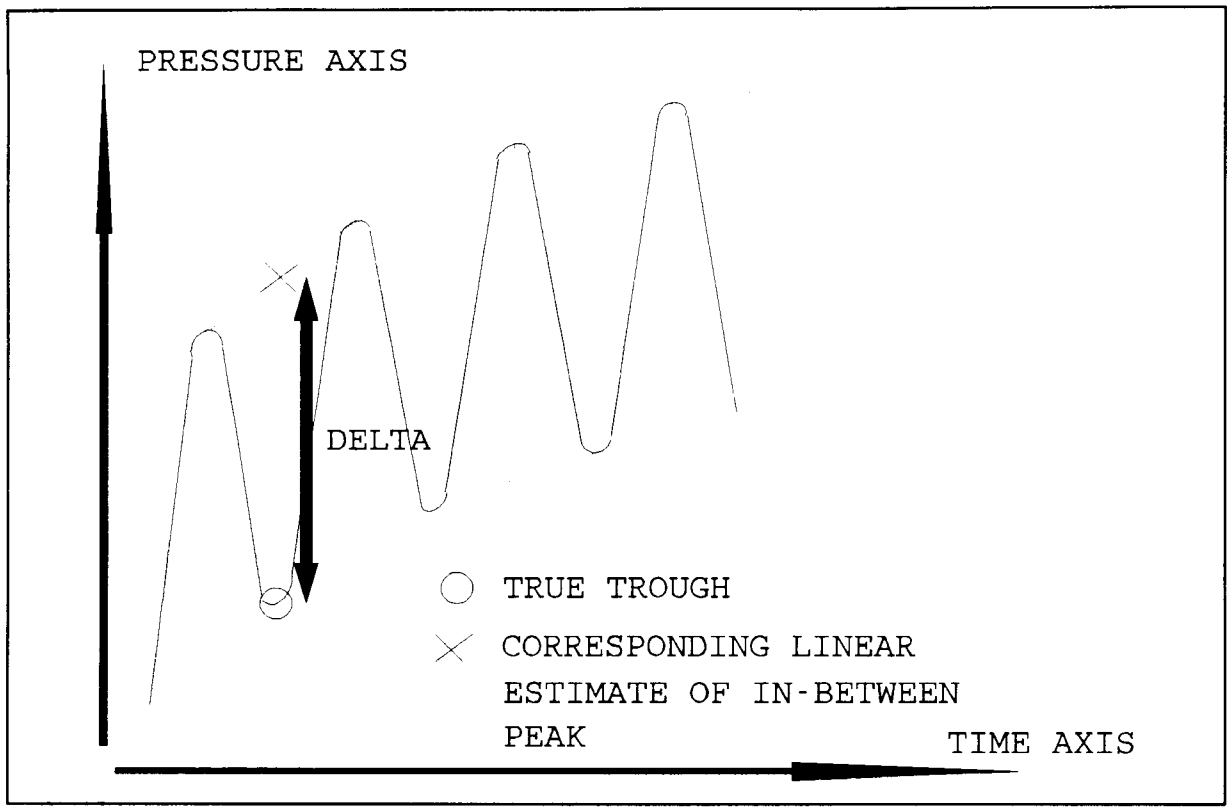

Figure 5.2 : Extraction of "deltas" using linear estimates.

5.4.2. Measure

The flow chart depicted in figure 5.3 describes the MEASURE function. This function enables the sampling of the pressure transducer voltages and the processing of the digital samples, and is described as follows:

1. A hardware check is performed. An "A/D card OK" flag, set during the "initialization" of the programme, is checked. If not set, the user is warned appropriately and measuring is disabled. In this case the measure function is terminated and the user is returned to the MENU.
2. If the flag is set, the user is prompted to ensure that the BODYBOX is not sealed, and that the piston mechanism is switched off. The differential pressure transducer is then sampled for a short sampling period of a second, during which the hardware bias or offset voltage is measured, averaged and displayed.
3. The operator or user is then prompted to instruct the subject

to enter the BODYBOX, seal the BODYBOX, switch the piston on and to press any key when ready. Barometric and differential pressure samples are then collected at a rate of 100 Hz. This data acquisition is continued until either the full complement of samples (22 seconds) have been collected or a keypress is detected. If a keypress is detected before the end of sampling, the sampling is terminated and the user is offered the choice of either redoing the sampling, or returning to the MENU.

4. Once the required amount of samples have been collected, the user is informed of such.

5. The barometric pressure samples are averaged and the atmospheric pressure, during sampling, is calculated and displayed.

6. The pressure "delta" extracting algorithm described earlier is then applied to the differential pressure samples. A "delta" window displays the pressure variations.

7. A mean value is calculated for theses "deltas" and the standard deviation which gives an indication of the quality of the measurement is calculated. The mean and standard deviation is displayed. The averaging serves as an effective filtering technique.

5.4.3. Compute

The flow chart depicted in figure 5.4 shows the COMPUTE function visually. It performs the final calculation of the body volume, density and percent fat and is described as follows:

1. A check is done to determine whether appropriate data exist in the main, global array (namely the differential pressure array).

2. If not, the user is instructed to either perform a measurement, or load a data file, and is then returned to the MENU.

3. Once the check proves affirmative, the programme calculates the subject's body volume, body density, and percentage body fat, displays these results and returns to the MENU.

4. For the volume calculation, the following expression is used

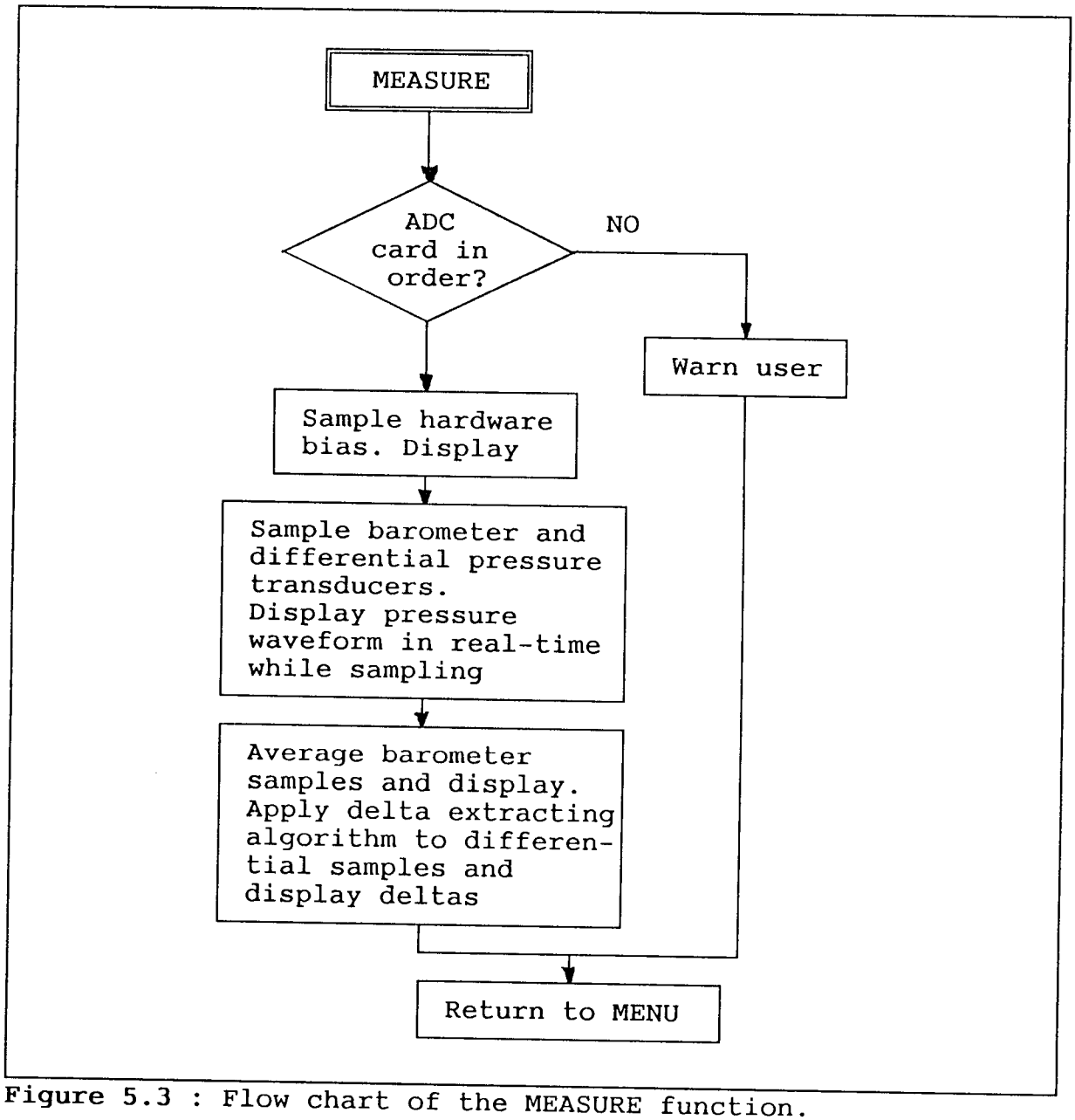

Figure 5.3 : Flow chart of the MEASURE function.

(for the derivation of this expression, see chapter 3):

$$V_B \doteq V_C - \frac{kP_C\Delta V}{\Delta p} - \frac{k+1}{2}\Delta V$$

where V_B is the subject's body volume in l, V_C is the container or BODYBOX volume in similar, ΔV is the stroke volume of the piston in similar, k is the specific heat ratio (a constant of 1.400 (unitless) is used), Δp is the above-mentioned "delta" in pressure in Pa, and P_C is the chamber pressure in Pa.

5. The body density is calculated as the subject's body mass

divided by his/her body volume.

6. The next expression shows how the percentage body fat is calculated, according to Siri, 1961. As a result of the simplifying assumptions mentioned previously regarding body density these results must be treated with caution. D_{BODY} is the subject's body density.

$$\%\ BODY\ FAT = 100\left(\frac{4.95}{D_{BODY}} - 4.50\right)$$

7. The body volume, density and percent fat is then displayed.

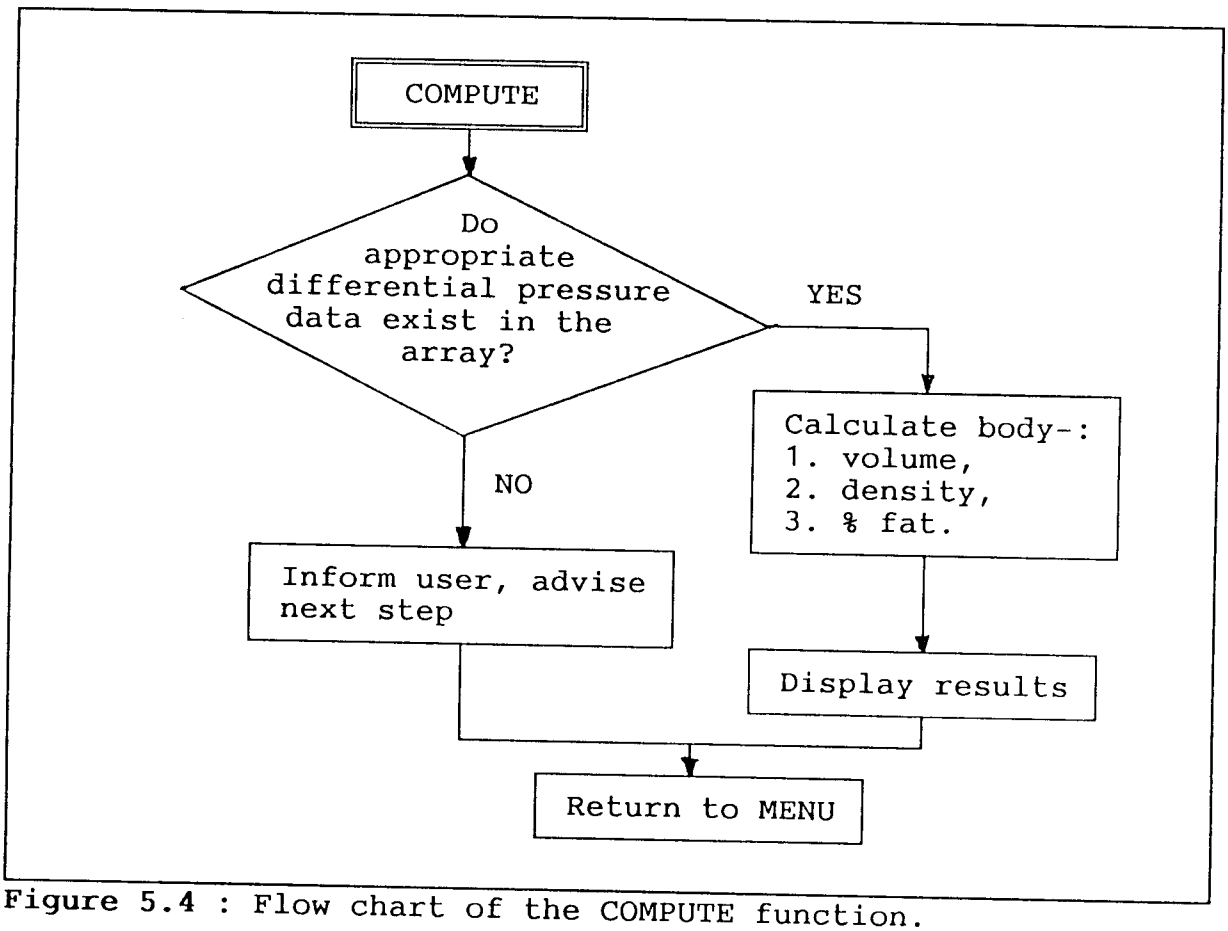

Figure 5.4 : Flow chart of the COMPUTE function.

5.4.4. Load

This function is depicted clearly in terms of a flow chart in figure 5.5. It enables the listing of files and permits the user

to load previously generated data files for re-analysis and is described as follows:

1. The user is prompted to save previous data, if desired.
2. Then the user is prompted to list all data files within a (sub)directory, if desired.
3. All data files with an extention ".DAT" are listed.
4. The user is then prompted to type in the name of the data file he/she wishes to retrieve and the file is loaded into the computer. If the specified file cannot be found, for any reason, the user is warned to this effect and he/she is prompted to either retry loading, or abort this operation and is returned to the MENU.
5. The data samples are collected from the file and read into the differential pressure array. The global variables or parameters, namely specific heat ratio (k), hardware offset, and body mass, are transferred in likewise fashion.
6. The contents of the loaded file are displayed in the graphics and the delta extracting algorithm is applied for analysis.

5.4.5. Parameters

The PARAMETERS function is depicted in figure 5.6. It allows the user to change the default values of the mentioned parameters at liberty and is described as follows:

1. The default, or current parameter values, namely specific heat ratio (k), mass, and barometer offset pressure, are displayed.
2. Simultaneously the user is prompted to either specify the parameter he or she intends to change, or to retain the current values.
3. The former action prompts for a new value, and if a valid value is received, the user is informed that it was accepted. If the user erred by typing a character rather than a number, he or she is instructed to retype the value. This loop is maintained until success is achieved.
4. After acceptance of a value, the user is shown what the new values are and again prompted to change, or not to change the values. The latter action once again displays the parameter

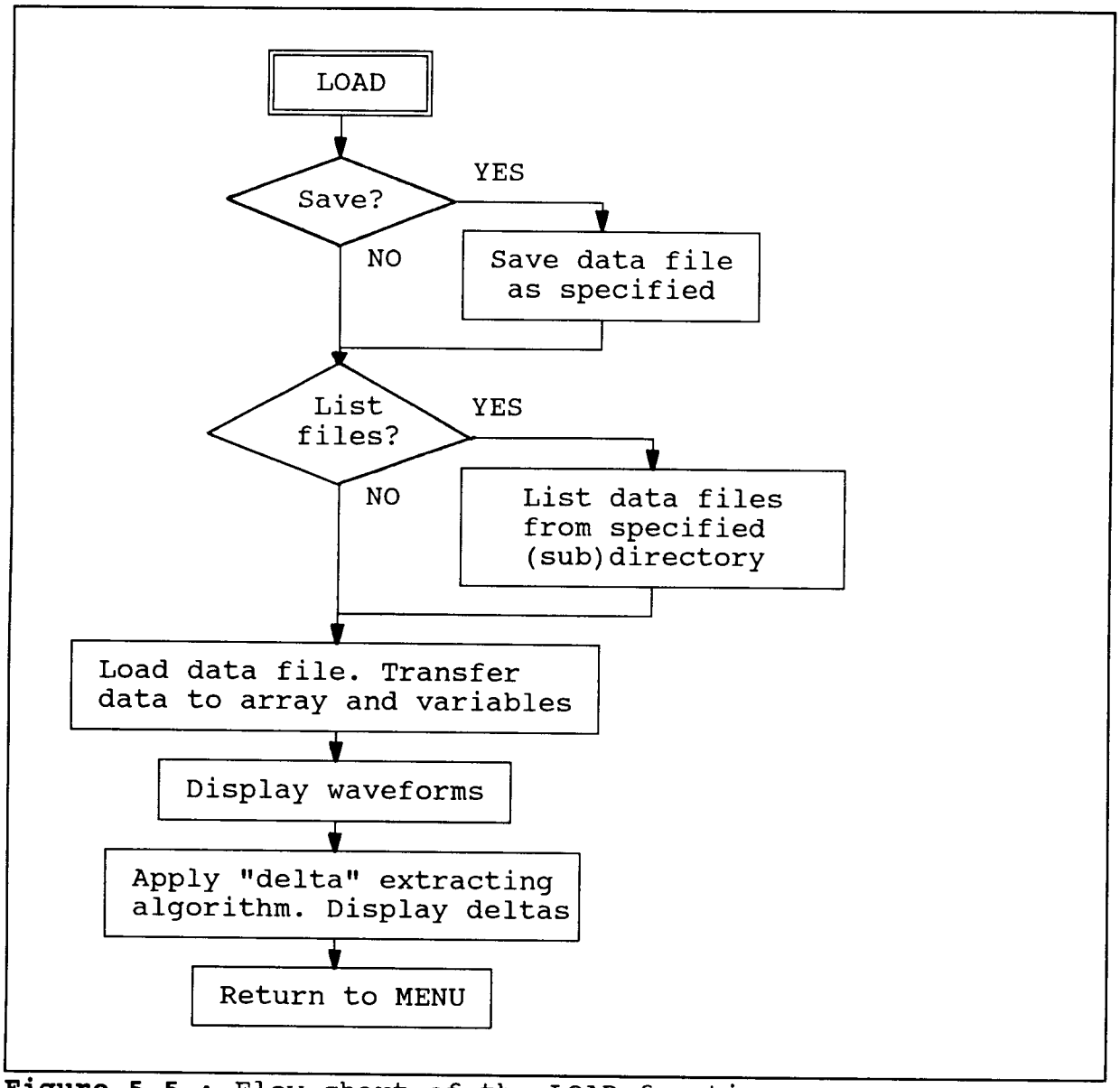

Figure 5.5 : Flow chart of the LOAD function.

values and returns to the MENU.

5.4.6. Save

A flow chart depicting the SAVE function appears in figure 5.7. This function enables the saving of the contents (raw sampled data and pertinent parameter values) of a measurement and is described as follows:

1. The user is prompted to enter a file name, which should

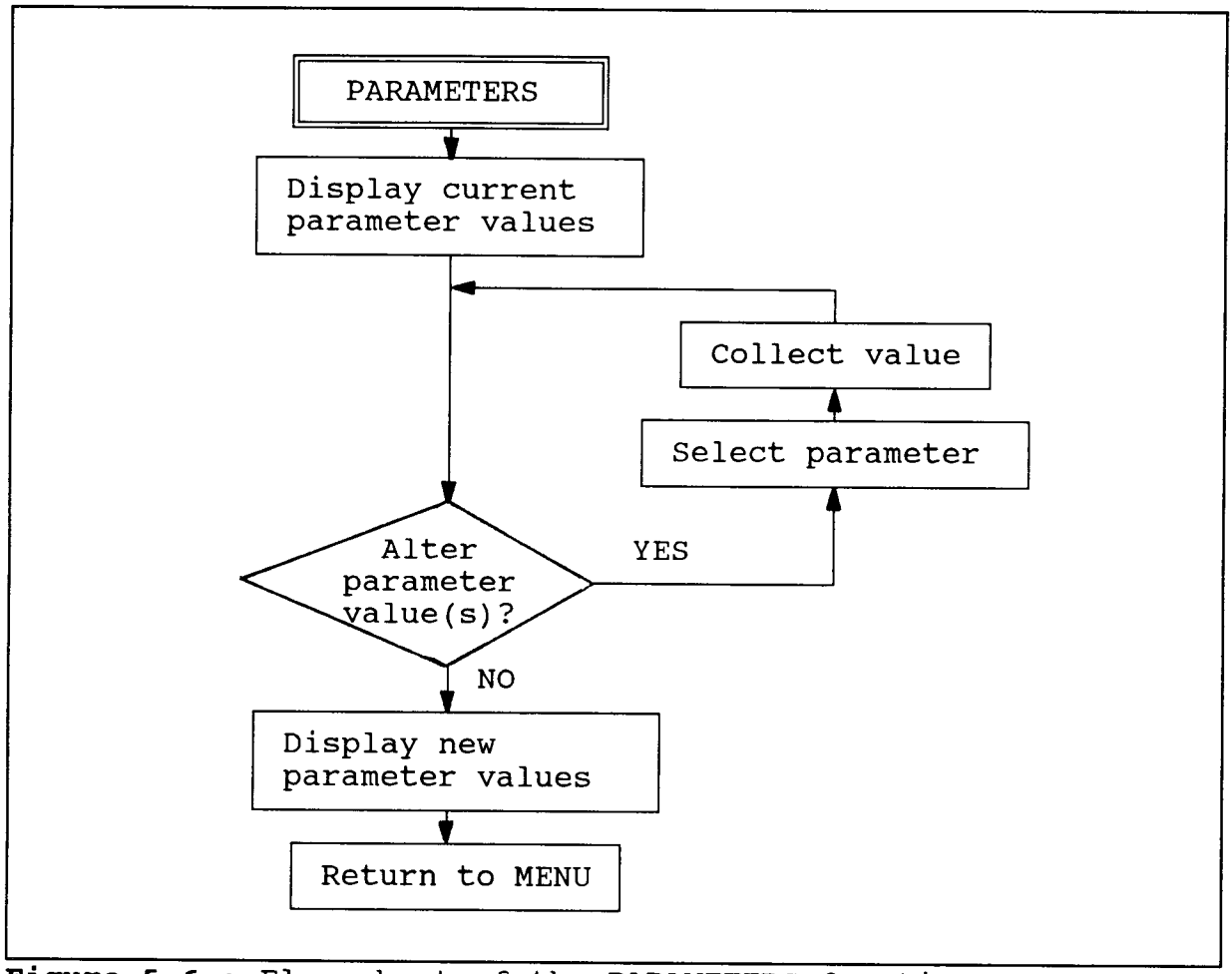

Figure 5.6 : Flow chart of the PARAMETERS function.

conform to DOS specifications (consist of up to 8 keyboard characters). An example of a file name which includes the drive and/or directory name is displayed on screen.

2. The name is collected as a string and an extension ".DAT" is automatically concatenated at the end of this string.

3. A test is run to establish whether a file by the same name already exists, or not. If a file by a similar name exists, the user may choose between overwriting the file, or typing in a new filename. If the entered filename does not conform to DOS, a flag is set. The flag is checked, and if found set, the user is prompted to either retry in which case the filename prompt is again given, and so on, or abort the saving procedure where the programme is returned to the MENU.

4. Once satisfactory conditions for writing a file are met, the following data are written sequentially into this opened file:

chronological array elements of the differential pressure array and four parameter values, namely specific heat ratio (k), atmospheric pressure, mass, and hardware offset. All values are integers, or in twin-byte form, which means the file is binary (not text).

5. Once this operation is finished the file is closed and the user is informed that the saving is completed.

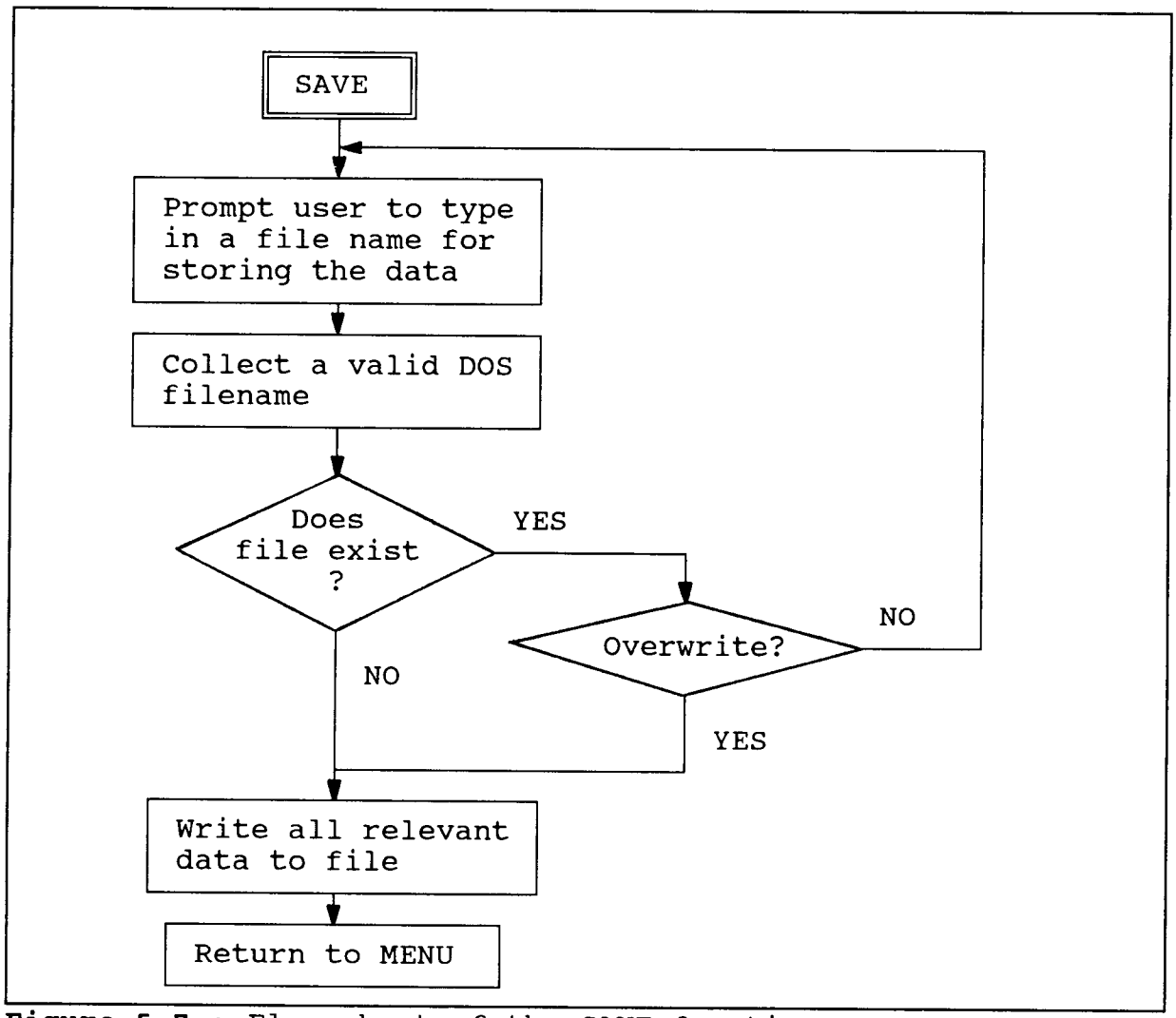

Figure 5.7 : Flow chart of the SAVE function.

5.4.7. Quit

The QUIT function is shown in figure 5.8. This function permits the user to escape or quit from the programme or measuring

procedure when desired.

Firstly the user is offered the choice to save the current data. If desired, the user indicates to this effect and the data is saved. Finally the computer screen is restored to the text mode, and the programme is halted.

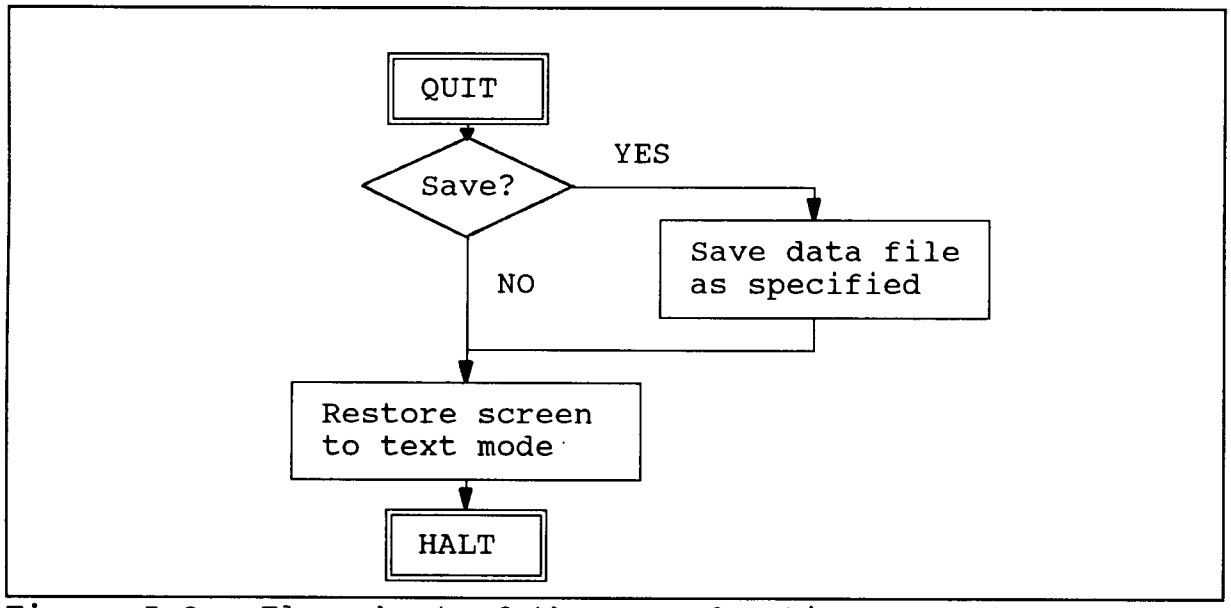

Figure 5.8 : Flow chart of the QUIT function.

6. ACOUSTIC MODELLING AND ANALYSIS OF THE BODYBOX

6.1. Introduction

In this chapter the acoustic behaviour of the BODYBOX is examined. If a natural resonance of the BODYBOX exists close to the operating frequency of the cycling piston mechanism, it may affect the linearity of the measuring system.

According to Helmholz the resonance frequency is proportional to the inverse square root of the chamber volume (Seto, 1971). Different chamber volumes caused by different displacing body volumes therefore shift the resonance causing a change in the acoustic behaviour at a fixed frequency. If the resonance frequency is close to the operating frequency and if the resonance is clearly defined (high Q-factor), different volumes will alter the system's gain significantly causing non-linear results. Consequently an electro-acoustic model of the BODYBOX is presented and is analyzed in theory and in practice.

6.2. Electro-acoustic model

Figure 6.1 represents the BODYBOX to be modelled whilst figure 6.2 is the equivalent electrical model. The atmospheric filtering chamber is excluded because a stable atmospheric pressure is assumed. The measuring chamber's compliance is represented by a capacitance, $C_{CHAMBER}$, calculated as: $C = V/(P_A k)$ (Bunn, 1980), where V is the volume (m^3), P_A is the atmospheric pressure (Pa) and k is the specific heat ratio (1.4 unitless) while the chamber leak is represented by a resistor, R_{LEAK}. The pipe between the piston and chamber has an inertance which is represented by an inductance, L_{PIPE}, calculated as: $L = \rho l/s$ (Bunn, 1980), where ρ is the density of air (1.205 kg/m^3), l is the pipe length (m) and s is the cross sectional area of the pipe (m^2). The pipe's resistance is represented by a resistance, R_{PIPE}, calculated as: $R = (1/s)SQRT(2\pi\rho\mu\omega/s)$ (Bunn, 1980), where μ is the coefficient of viscosity of air ($1.78*10^{-5}$ Ns/m^2) and ω is the

angular velocity (cycling speed of piston) ($\omega = 2\pi f$, f = frequency in Hz). The pressure developed by the piston is represented by an AC voltage of V_{PISTON} while the output differential pressure as seen by the transducer is represented by an output voltage of V_{OUT}. The tube connecting the differential pressure transducer to the chamber has an inertance (inductance) of L and a resistance of R. The ambient or atmospheric pressure is represented by a DC voltage source, E_{ATM}, which appears in series with each branch.

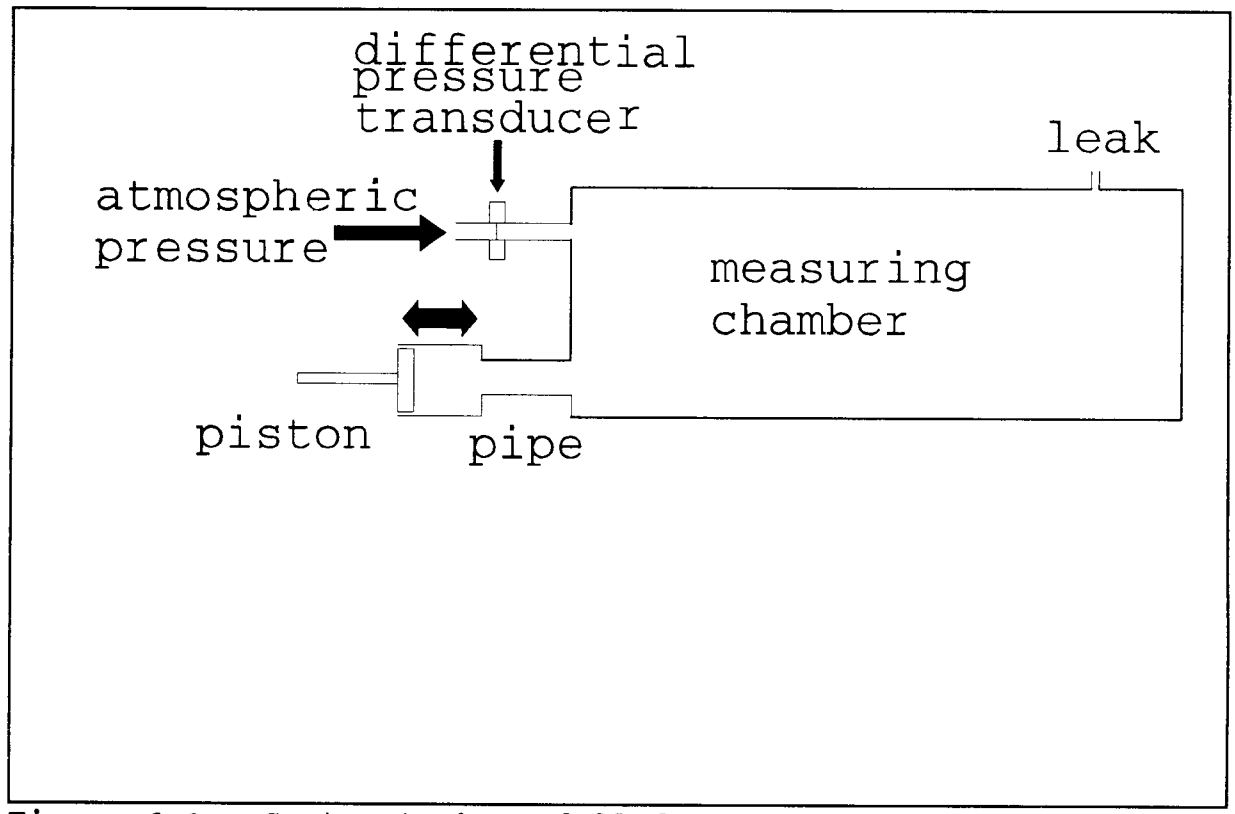

Figure 6.1 : System to be modelled.

In order to simplify the model in figure 6.2 the components indicated by *s are omitted in the model presented in figure 6.3. The leak resistance is considered as infinity while the transducer interconnecting tube's resistance and inertance is considered as zero. The atmospheric "DC voltage sources" are omitted because only the dynamic (AC) response is of interest for analysis of the acoustic behaviour.

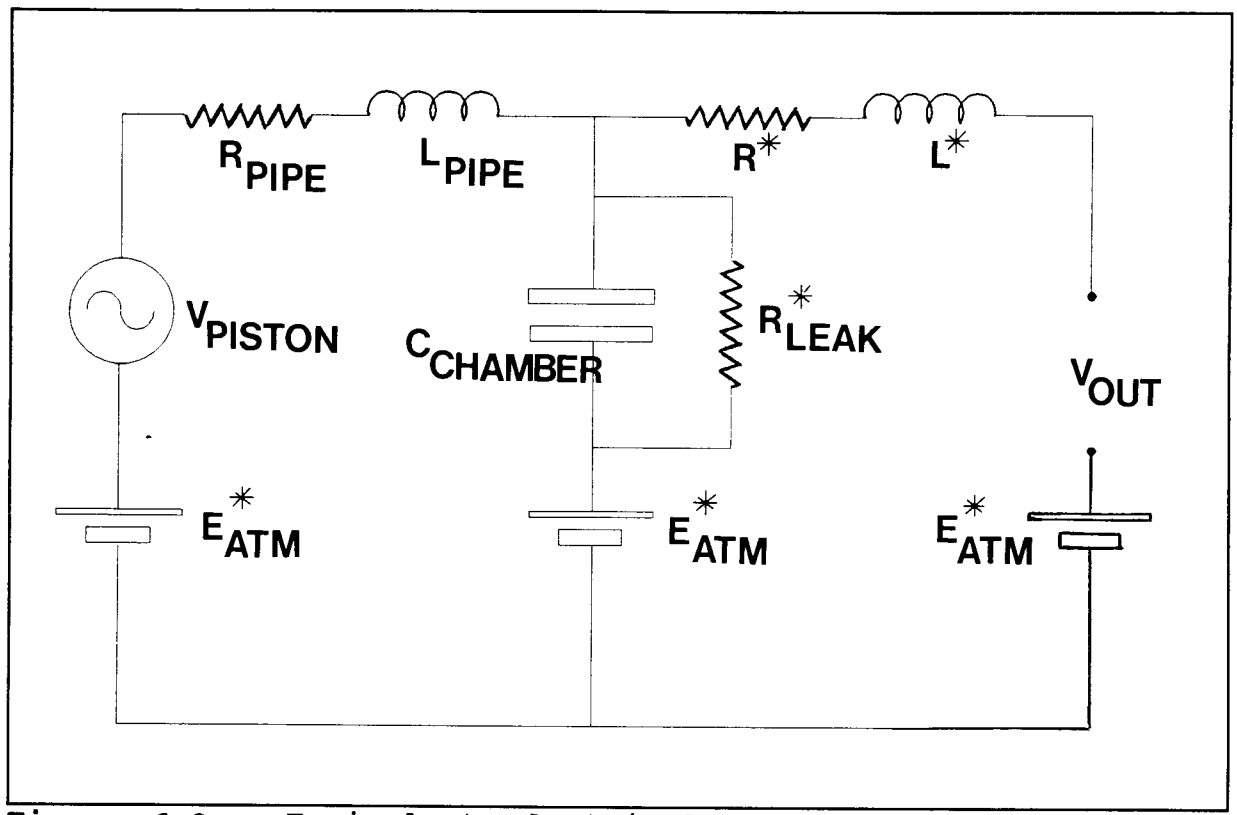

Figure 6.2 : Equivalent electrical model. The *s represent components omitted forthwith.

The transfer function of the equivalent model in figure 6.3 is:

$$H(j\omega) = \frac{V_{OUT}}{V_{IN}} = \frac{1}{1+j\omega RC-\omega^2 LC} \qquad (1)$$

The magnitude or gain is thus:

$$GAIN\{H(j\omega)\} = |H(j\omega)| = \frac{1}{\sqrt{\omega^4 L^2 C^2+\omega^2(R^2C^2-2LC)+1}} \qquad (2)$$

This leads to a resonant frequency (in Hz) of:

$$f_0 = \frac{1}{2\pi\sqrt{LC}} \qquad (3)$$

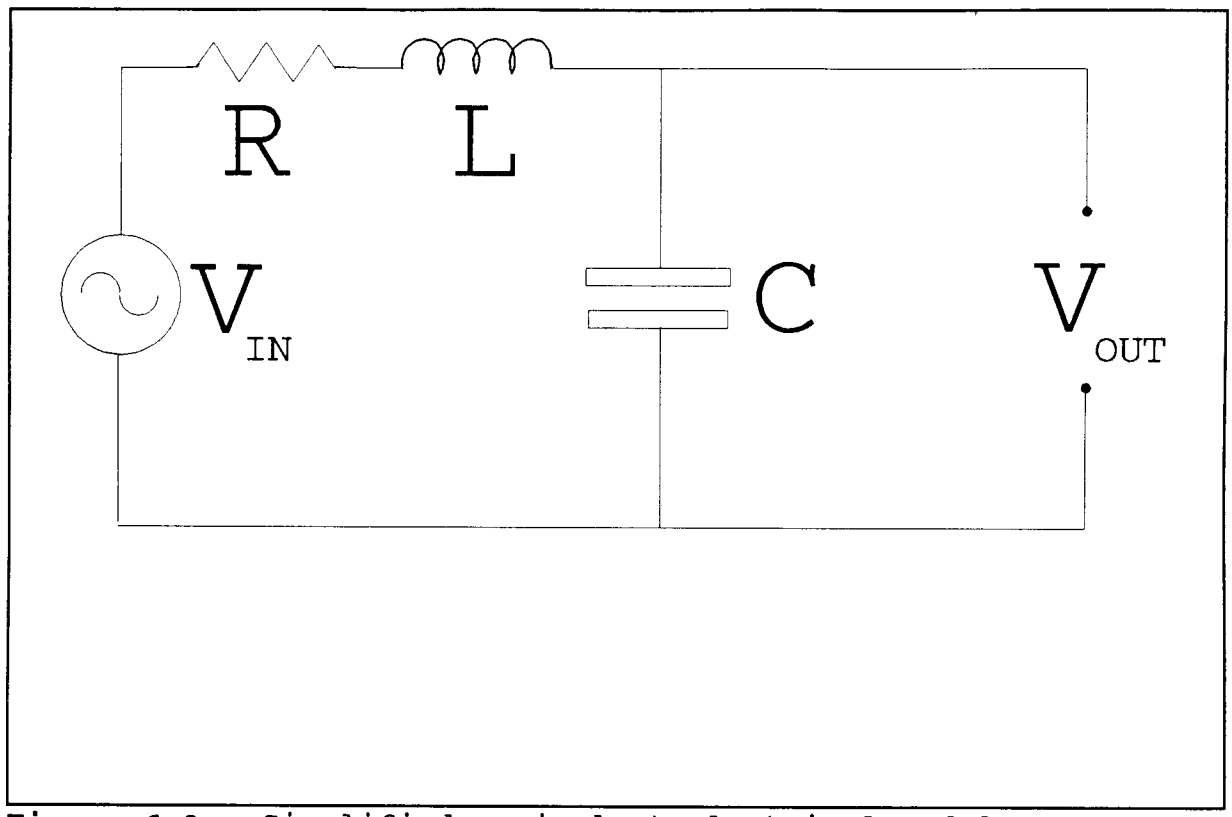

Figure 6.3 : Simplified equivalent electrical model.

6.2.1. Theoretical acoustic analysis

Figure 6.4 represents the theoretical response of the model in figure 6.3 for different values of R (10k, 20k, 40k, 60k). The values of R, L and C arise from the BODYBOX physical dimensions and are calculated at the Helmholz resonance frequency of 1.2 Hz. They are $6.68*10^{3}$ Ohm (not used in graph), $5.95*10^{3}$ Henry and $2.75*10^{-6}$ Farad, respectively.

6.2.2. Discussion

From figure 6.4 it is clear that increasing the resistance flattens the resonance peak. A change of the compliance as caused by a different chamber volume (effected by different displacement volumes) as well as a change of the inertance shifts the resonant frequency inversely (see equation (3)). This implies that any volume displacement, such as a subject in the

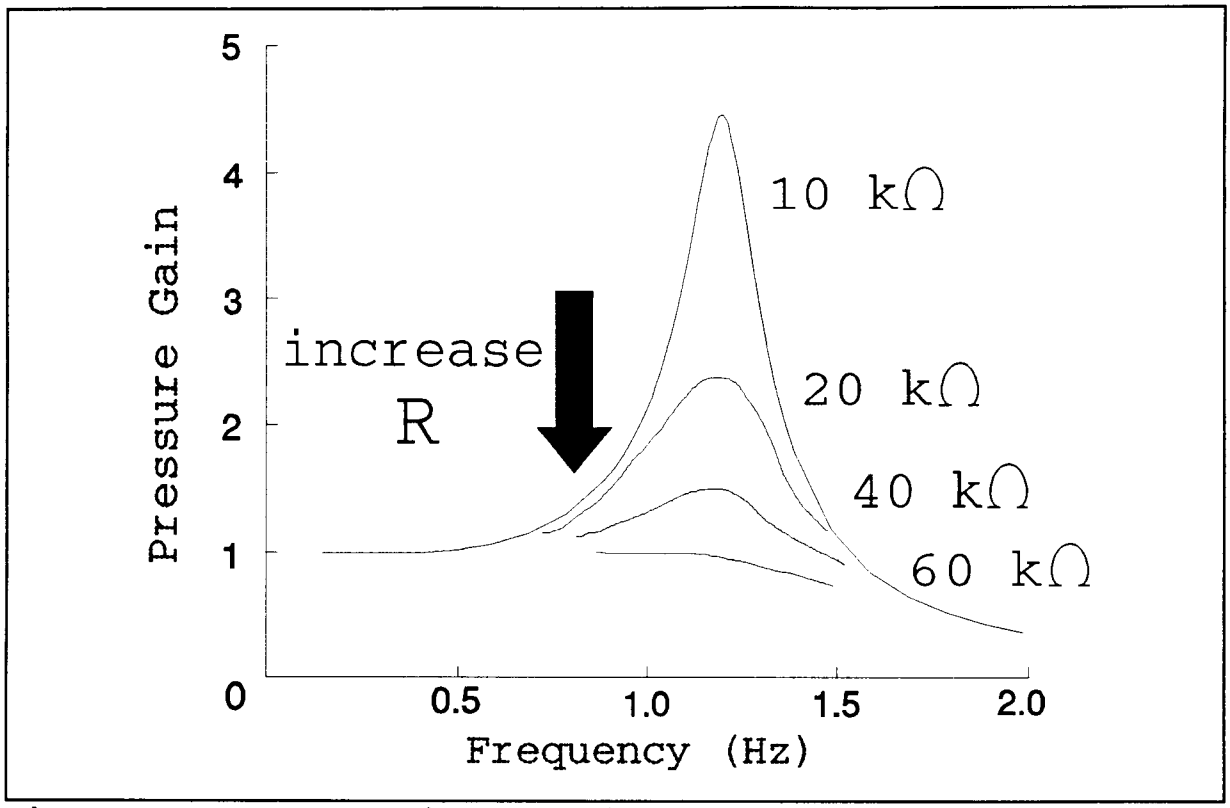

Figure 6.4 : Theoretical magnitude-frequency response of the simplified model at different R values.

chamber, will cause an increase in the resonance frequency of the system. Since the theoretical resonant frequency of the system (1.2 Hz) is close to the driving frequency it was considered necessary to measure the acoustic behaviour of the system. This analysis is presented in the following section.

6.3. Practical acoustic analysis

6.3.1. Materials and methods

In the original system the piston mechanism is driven by a fixed-speed AC motor. To control the speed of the mechanism and therefore perform a frequency response analysis of the system, a DC motor with a variac (variable output transformer) and rectifier was used. To ensure that the response of the physical (acoustic) system was not affected by the electronic filter in the transducer interface, this filter was removed during the

course of the acoustic analysis. Pressure variations ("deltas") sampled by the system were analyzed over a range of piston frequencies (0.25 - 1.5 Hz) in the region of the expected resonance as follows:

6.3.2. Results

The frequency response of the BODYBOX has been measured and is presented in figure 6.5.

6.3.3. Discussion

No clearly defined resonance appears. The response corresponds to that of the theoretical model with a relatively high acoustic resistance R (60 k Ohm). Such a response is also typical of a second order low pass filter.

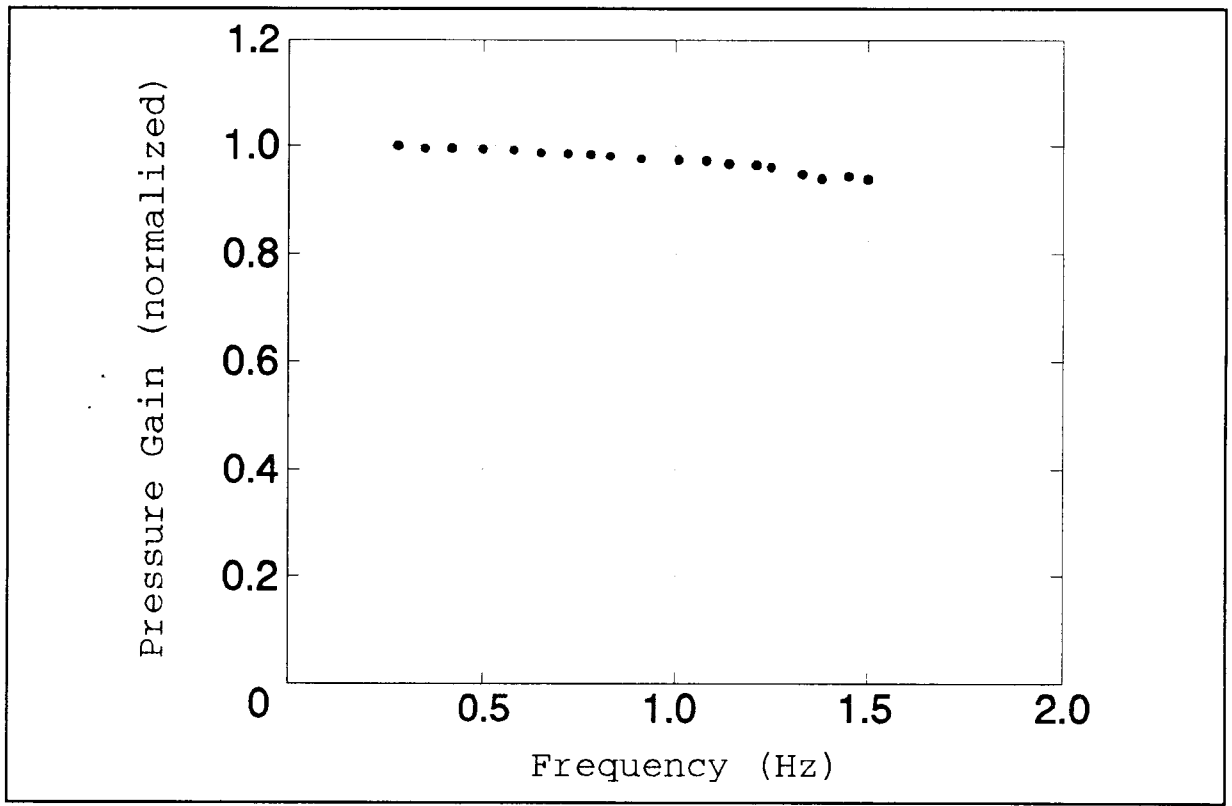

Figure 6.5 : Measured magnitude-frequency response of the BODYBOX (electronic filter excluded).

6.4. Conclusion

The acoustical analysis has shown that the linearity of the measuring system is not affected because a negligible change in gain or output has been found to occur in the region of the operating frequency (0.53 Hz).

7. FUNCTIONAL EVALUATION OF THE BODYBOX

7.1. Introduction

This chapter deals with the functional evaluation of the BODYBOX and is divided into four parts namely influencing factors, calibration of the BODYBOX, verification for neglecting lung volume correction and volume measurements on human subjects.

7.2. Influencing factors

Various factors, like pressure leaks, noise originating from the pressure transducers and associated circuitry, fluctuations in atmospheric pressure, light, heat and humidity, which influence the measuring accuracy and capability of the BODYBOX have been examined and are discussed now. In chapter 3 pressure leaks, heat and humidity were discussed theoretically.

7.2.1. Pressure leaks

The varnished wooden lid distorted with time causing a degradation of the seal. Hence an additional rubber seal has been fitted. This improved the pressure leak time constant from 7.6 to 92 s which minimized the acoustic feedback of atmospheric noise across the differential pressure sensor and increased the overall pressure gain of the BODYBOX, the latter requiring a correctional adjustment in the software.

7.2.2. Noise

Noise originating from the differential pressure transducer and associated circuitry has been analyzed. The absolute (barometric) pressure transducer is not dealt with since the sensitivity of this variable (atmospheric pressure) with respect to body volume is small compared to that of the pressure variations caused by the cycling piston.

light trap was installed inside the chamber, at the entrance to the differential pressure transducer, and all tubes connected to the transducers were painted black. Pressure drifting caused by these effects were subsequently not detected.

7.2.5. Heat

Temperature affects the system in two main ways:
1. Transducers: Although temperature compensation is built into the pressure transducers (see the technical specifications in the

The maximum noise voltage encountered at the output, as measured by an oscilloscope, was approximately 2.5 mV, peak to peak. This represents a "pressure error" of 0.14 Pa (which translates to a volume error of 0.13 l for a 70 l man), compared to a typical pressure variation of 350 Pa (S/N = -68 dB).

7.2.3. Fluctuations in atmospheric pressure

Atmospheric pressure fluctuations may be divided into slow and rapid components. The slow, or naturally occurring meteorological changes are continuously monitored by the absolute or barometric pressure transducer, which is integrated into the system. The rapid, often significant components are caused by the opening/closing of doors in the vicinity of the BODYBOX and are also caused by gusty weather conditions, the pressure changes of which are transmitted across window panes.

The outer port of the differential pressure transducer communicates with the outside (atmosphere) via an acoustic filter which consists of a rigid container of comparable volume to the measuring chamber and a long thin tube as shown in figure 4.1. This combination acts like a second order low pass filter. The improvement in noise was a reduction from 1.0 to about 0.14 Pa (including the electric noise of the circuitry) as measured by an oscilloscope and converted to pressure. This translates to a volume error of 0.13 l (70 l man).

7.2.4. Light

prepared. The empty containers weighed 1.14 kg each (without cap). From the density of the plastic material of 0.94 g/cc the volumes of each container "shell" was estimated (average of 1.209 l). Accurate fluid measuring containers were used to make up each volume unit to a volume of 27.00 l by adding tap water (excess gasses and bubbles flushed by standing several days).

The BODYBOX could then be calibrated against combinations of these known volumes (0, 27, 54, 81, and 108 l) by measuring each combination three to four times and averaging.

7.3.2. Results

The results of a typical calibration are presented in table VII.I. whilst volume error is plotted in figure 7.1.

Table VII.I : A typical volume calibration (all values in l).

TRUE VOLUME	MEASURED VOLUME	ERROR
0.0	3.1	+3.1
27.0	30.0	+3.0
54.0	55.7	+1.7
81.0	81.3	+0.3
108.0	107.2	-0.8

7.3.3. Discussion

A smooth monotonic transition between these estimated volumes over the entire volume range (0 to 108 l) is assumed. Hence corrections are made to volumes as estimated by the BODYBOX according to linear interpolations of these calibration "error volumes". However, a non-linear system can always be "linearized" as long as the non-linearity is known.

Day-to-day calibrations give different results. A possible explanation is that a slight variation of the specific heat

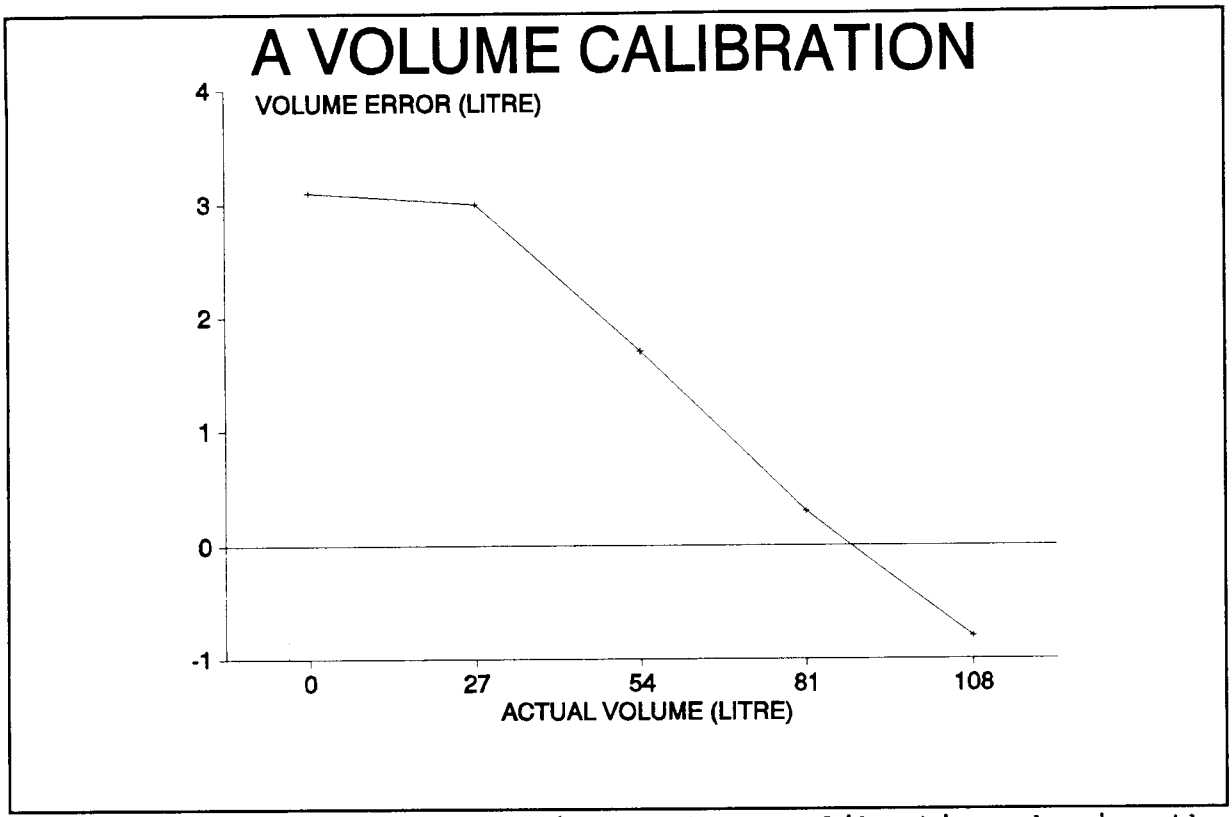

Figure 7.1 : A plot of a typical volume calibration showing the volume error.

ratio, k, which may be caused by humidity variations from day to day affects calibrations differently. By theoretically changing k very slightly (for instance increasing k from 1.400 to 1.401) the calibration error curve will shift in relation to the change (in the example at 0 l the error will be elevated by 0.28 l and at 120 l by 0.19 l between which the slope will be nearly-linear). Frequent calibrations of the BODYBOX is thus required.

7.4. Verification for exclusion of lung volumes

Previous investigators have assumed that, unlike the case for the underwater weighing technique, residual volume measurements are not required as the lung can be considered to be in acoustic communication with the chamber and thus form part of the remaining chamber volume (Gundlach and Visscher, 1986). If the diaphragm is sufficiently compliant and/or the glottis is kept open this assumption should be valid. Tests were carried out to

determine to what extent relatively rigid air-filled containers (viz. the empty plastic containers used for calibration) communicated with the chamber. Tests were also carried out on two human subjects whose body volume was measured whilst breath holding at both total lung capacity (TLC) and residual volume (RV). Volume differences equal to the subjects' vital capacities (TLC - RV : between 4.5 to 9 l) were expected if no communication was present.

7.4.1. Materials and methods

Empty plastic containers as described in paragraph 7.3 were used for this test. These containers with 1 mm thick walls are reasonably rigid due to their construction. The empty container "shells" each have an estimated volume of 1.2 l totalling 2.4 l whilst the closed (sealed) containers had a combined estimated volume of 55.0 l. A full calibration as described (7.3) was first carried out. Two open containers (empty) were then placed inside the chamber whereafter the volume was estimated four times by the BODYBOX. This test was repeated for the same two containers, this time closed by proper sealing caps.

7.4.2. Results

The results of the test on the containers are presented in table VII.II and those of the test on the 2 subjects in table VII.III. No significant difference was detected in the pressure variations measured at both lung volumes in both subjects.

7.4.3. Discussion

The test showed that only 66 % of the expected volume was "seen" by the BODYBOX. Thus the remaining 34 % of the volume, constituting 35.6 % of the total enclosed gas volume, was not "seen" and hence communicated with the inside of the chamber.

Table VII.II : A comparison of the opened and closed container volumes (all values in litre).

OPENED CONTAINERS			CLOSED CONTAINERS		
Expected	Estimated	Corrected*	Expected	Estimated	Corrected*
2.4	4.00		55.0	38.10	
	3.84			38.14	
	3.87			37.97	
	3.80			37.79	
	----			-----	
Mean:	3.88	2.5		38.00	36.3

* denotes the correction made to the mean of the estimates according to the preceding calibration

Table VII.III : A comparison of the breath holding body volumes of 2 subjects at TLC and RV (in l).

SUBJECT #	VC	VOLUME @ TLC	VOLUME @ RV
A	7.7	64.4	63.9
B	4.3	61.9	61.3

VOLUME @ TLC/RV : BODYBOX assessed volume with subject at total lung capacity or residual volume, respectively (average of 3 measurements each).
VC : Vital capacity measured with lung function equipment.

The enclosed gas spaces in the reasonably rigid containers communicated partially with their surroundings and the assumption can be made that a similar phenomenon occurs when placing a human inside the chamber. Human chest walls (especially the diaphragm) are far less rigid and will communicate with the chamber to a higher degree. Communication between the lungs and inside the chamber may be further enhanced by an open glottis and direct communication via the airways. Gastro-intestinal gasses should also, for the same reason, communicate. Evidence of non-communication in human subjects could not be detected and the assumptions used by Gundlach and Visscher (1986) appear valid.

7.5. Body volume tests on human subjects

7.5.1. Materials and methods

A small population of eight healthy, young and co-operative adult human subjects were measured in the BODYBOX, whereafter they were measured by using three other body composition methods, namely underwater weighing (UWW), skinfolds (SKF), and bioimpedance analysis (BIA). A detailed description of the BODYBOX procedure follows. Details and data of the other methods appear in the appendices.

Preparation:
Before measurements are started the BODYBOX is allowed sufficient warm-up time. The barometer is calibrated against an accurate source obtained from the regional weather buro (about 10 to 15 km away) and corrected to allow for the change in height. Heights are obtained from accurate land surveying maps. The difference in height is estimated at approximately 10 m. A single telephone call is necessary to obtain the barometric pressure reading which is then corrected by +0.12 kPa. The BODYBOX is then calibrated against a set of known volumes (see calibration, 6.3). Prior to measurement the subjects are properly informed about the procedure.

Measurement:
Each subject, wearing minimal clothing (usually a well-fitting bathing costume), is instructed to enter the perspex cylindrical chamber feet-first, to pull up the legs slightly, and to lie down on his/her back as comfortably as possible. He/she is asked not to breathe into the chamber, as this could introduce additional humidity into the system. The snorkel, with fitted discardable mouthpiece, is immediately brought to the subject's mouth so that he/she can comfortably breathe through it and out of the system. The controlled leak is open at this time to facilitate pressure equalization with the outside while closing the lid and thereafter, due to body heat. The lid is then closed thoroughly

by securing the latches.

The operator and the subject are able to verbally communicate through the chamber wall. The subject is allowed a few moments to relax and become familiarized with the chamber. Then he/she is instructed to hyperventilate lightly to allow for an adequate period of breath-holding (approx. 22 seconds), after which he/she will start holding breath at an elevated lung volume, remove the mouthpiece, and block the snorkel end with the rubber bung. From this point the subject is requested not to move or breathe until completion of the measurement when the operator gives the subject a hand signal to show him/her to remove the bung and refit the mouthpiece for breathing. During the approximately 22 seconds of measurement the operator follows a sequence of actions:

- measure the bias voltage of the sensor interface (mean of the sampled value over 1 second),
- seal off the controlled leak,
- start operation of the piston mechanism (crank previously centred),
- start the sampling of the chamber pressure and the barometer pressure signals,
- wait for the sampling to be completed (approx. 18 seconds).

After completion of sampling the computer starts processing the samples and displays the pressure variations. The operator may then save the data of this measurement on disk. These measurements are repeated until satisfactory repeatability is achieved. A third party is always on standby to ensure smooth running and subject safety.

7.5.2. Results

By applying the previously derived expression relating volume to the pressure variation, atmospheric pressure, and other physical, fixed constants, the displaced volume for each subject is estimated. From this estimate, a calibration correction is made. Body density is calculated by dividing body weight by volume.

By employing Siri's (1961) expression relating % body fat (%BF) to body density the %BF is estimated (see Introduction with cautionary note). The volume estimates of the eight subjects are presented in table VII.IV.

Table VII.IV : BODYBOX estimates of body volume, body density and percent body fat.

SBJ #	DeltaP Mean (Pa)	PAtm (Pa)	VOLUME Est. (l)	VOLUME Corr. (l)	BW (kg)	BD (g/cc)	%BF (%)
1	354.135	101790	68.93	68.50	71.3	1.041	25.6
2	341.145	101790	56.73	55.66	57.5	1.033	29.2
3	341.875	101800	57.41	56.37	58.7	1.041	25.3
4	351.290	101800	66.31	65.74	67.5	1.027	32.1
5	355.565	102010	69.52	68.58	74.3	1.083	6.9
6	354.935	102010	68.95	67.99	72.5	1.066	14.2
7	344.540	102010	59.29	57.78	62.8	1.087	5.4
8	366.755	102010	79.27	78.89	83.5	1.058	17.7

Key to table:

SBJ #	Subject number;
DeltaP	Mean pressure differential inside BODYBOX, after 10 cycles;
DeltaP (Mean)	Mean DeltaP;
PAtm	Atmospheric (barometric) pressure;
VOLUME (Est.)	Estimated volume, before calibration correction;
VOLUME (Corr.)	Corrected volume, after calibration correction;
BW	Body weight;
BD	Body density;
%BF	Percent body fat, according to Siri (1961).

The BODYBOX estimates of body volume is compared to the underwater weighing estimates and is presented in table VII.V. Figure 7.2 shows a comparison, by way of a linear regression, between the BODYBOX and the UWW volume estimates.

Table VII.V : A comparison of estimated volumes, as collected from the BODYBOX and underwater weighing methods (all values in l).

SBJ #	UWW	BOX
1	67.4	68.5
2	54.9	55.7
3	57.9	56.4
4	65.0	65.7
5	69.1	68.6
6	68.5	68.0
7	58.9	57.8
8	78.6	78.9

Key to table:

SBJ # subject number;
UWW underwater weighing estimates;
BOX BODYBOX estimates (system under consideration).

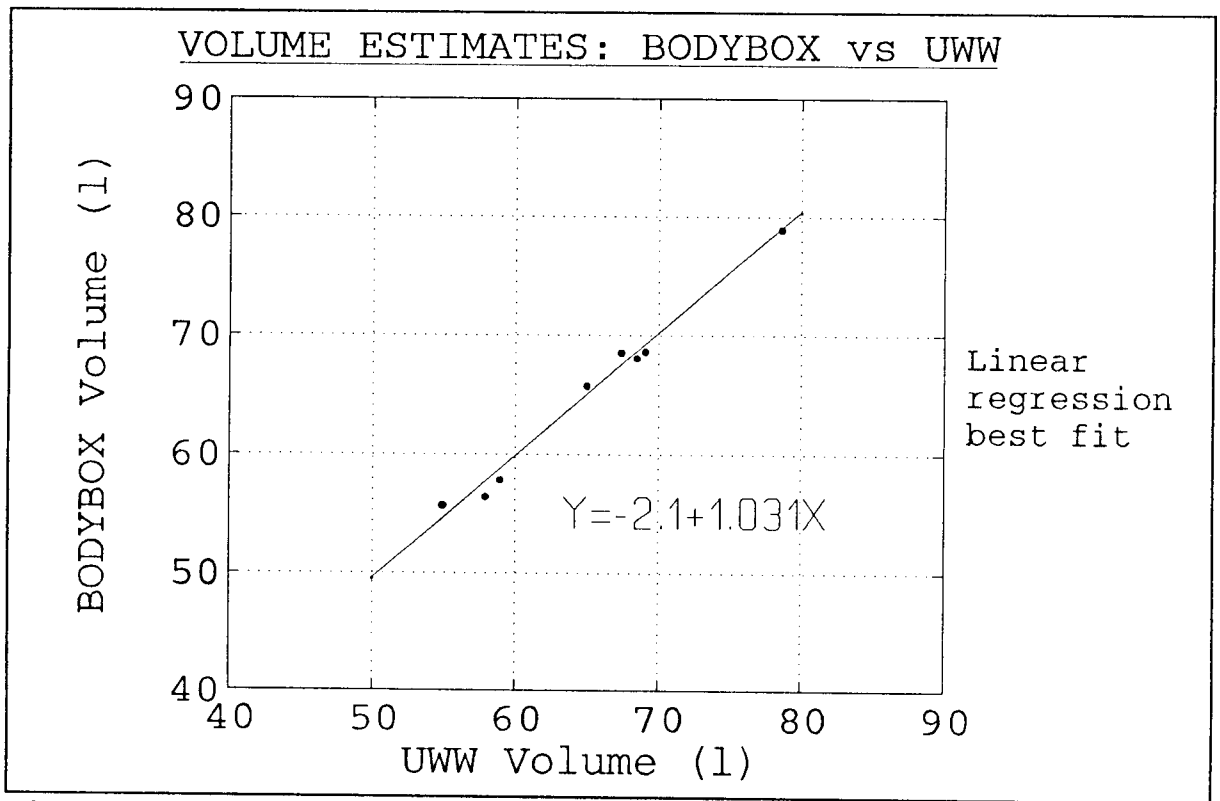

Figure 7.2 : A comparison between the BODYBOX and the UWW volume estimates.

A simple linear (least squares) regression was performed and the correlation coefficient was calculated, in order to evaluate the BODYBOX, when comparing it to the underwater weighing method.

Table VII.VI provides these statistics.

Table VII.VI : Statistical analysis performed as a comparison between the BODYBOX and the underwater weighing method (in terms of volume).

METHOD COMPARED	REGRESSION EQUATION	CORRELATION COEFFICIENT
BOX(Y) vs UWW(X)	Y = -2.100 + 1.031X	0.9930

Table VII.VII provides a compilate of percent body fat as estimated by the different methods.

Table VII.VII : A comparison of percent body fat estimated by the different methods.

SBJ #	BOX	UWW	SKF	BIA1	BIA2
1	25.6	16.6	16	20	13.4
2	29.2	28.6	23	26	23.6
3	25.3	32.7	27	27	25.7
4	32.1	26.7	30	33	29.0
5	6.9	10.4	8	11	8.7
6	14.2	18.5	12	13	9.5
7	5.4	14.6	10	18	12.7
8	17.7	16.0	11	14	12.0

Key to table:

SBJ # subject number;
BOX BODYBOX estimates;
UWW underwater weighing estimates;
SKF skinfold estimates;
BIA1 bioimpedance analysis estimates (RJL instrument);
BIA2 bioimpedance analysis estimates (Bodystat 500).

Repeatability between trials with respect to volumes showed a standard deviation with a worst case of 0.26 %. The standard error of estimation is 0.937 l which represents a typical error of 1.44 % (with respect to a body volume of 67 l).

7.5.3. Discussion

The BODYBOX appears to compare in close agreement to the reference method, namely underwater weighing. Regressions performed between the BODYBOX and the other methods, in terms of percent fat mass (not shown), does not appear as favourable as regressions in terms of volume due to the increased sensitivity to error being about 5-fold, according to Siri (1961) (another cautionary note). The standard estimation error of 0.94 l compares well with that achieved by a previous group of investigators (Gundlach, Nijkrake and Hautvast, 1980) who also used a plethysmographic method for determining human body volumes.

8. CONCLUSIONS AND RECOMMENDATIONS

8.1. Conclusions

A low-cost, mechanically and operationally simple and reliable human body volume measuring device has been built. This device, namely the BODYBOX, correlates highly ($r = 0.993$) with the standard underwater weighing method and exhibits a low standard error of estimate (0.94 l) and is thus an effective substitute for that method. Subjects have reported a vast improvement in comfort, in comparison to the underwater weighing technique.

The relative accuracy of the system is basically a consequence of the following:

1. The BODYBOX is free from resonance in the vicinity of the driving frequency (0.53 Hz). This ensures linearity of measurement.
2. It has been shown that the lung volume and gastro-intestinal gas volume of the subject are excluded from the body volume (i.e. becomes part of the chamber volume), when using the BODYBOX.
3. Frequent calibration of the BODYBOX ensures "linearization" of the device.

8.2. Recommendations for further research and development

It is recommended that, for further validation of the BODYBOX, the limits of human body volumes be expanded from the present 55 - 78 l to, say, 30 - 150 l. Further research and development may also be afforded to the following aspects:

1. Electronics: Special emphasis could be placed on the temperature stability of sensitive components like instrumentation amplifiers and pressure transducers. Low temperature coefficients will require less frequent calibration.
2. Environment: An alternative to low temperature coefficients is to house the system in an air-conditioned room.
3. Materials: The ends of the measuring chamber could be constructed of a rigid, non-porous material with insulatory

properties such as thick acrylic (perspex).

4. Piston mechanism: In order to improve on the semi air-tight seal of the device, a rolling-sock-type seal could be utilized instead of a piston with a rings-and-lubricant seal.

5. Measuring chamber: For assessing the frail and obese the chamber could be constructed of larger dimensions and could be fitted with a rigid trolley bed to ease entering and exiting.

6. Measuring procedure: This can be substantially improved by:

- shortening the measuring period from 18.5 (10 cycles) to 5 seconds (3 cycles) (this should enable paraplegics and the frail to be measured);
- incorporating a calibrating option in the software;
- incorporating a mechanism which automatically stops the conrod of the piston at a predetermined position, immediately after the measuring period;
- using a solenoid-controlled leak for pressure equilibration, instead of by hand;
- adding a solenoid-type release mechanism on the lid which could be activated from both inside and outside the chamber.

In general the device should prove to be a useful alternative to the underwater weighing technique for measuring body volume. By reducing the breath hold period to 5 seconds, by increasing the dimensions and by incorporating a trolley bed it should be possible to measure frail, obese and paraplegic subjects.

REFERENCES

BEHNKE AR, FEEN BG, WELHAM WC.
1942.
The specific gravity of healthy men.
The Journal of the American Medical Association, 118(7):495-501.

BROZEK J, GRANDE F, ANDERSON JT, KEYS A.
1963.
Densitometric analysis of body composition : Revision of some quantitative assumptions.
Annals of the New York Academy of Sciences, 110(Sept):113-140.

BUNN AE.
1980.
Theory and physiological applications of pressure waves in compliant tubes.
Stellenbosch, South Africa: University of Stellenbosch.
pp.19-21. PhD Dissertation.

BUSKIRK ER.
1961.
Underwater weighing and body density : a review of procedures.
pp.90-107 In: Brozek J, Henschel A, eds. Techniques for measuring body composition.
Washington, DC : National Academy of Sciences-National Resource Council.

BUSKIRK ER, MENDEZ J.
1984.
Sports science and body composition analysis : emphasis on cell and muscle mass.
Medicine and Science in Sports and Exercise (Baltimore), 16(6):584-595.

DESKINS WG, WINTER DC, SHENG H-P, GARZA C.
1985.
An acoustic plethysmogragh to measure total infant body volume.
Journal of Biomechanical Engineering, 107(4):304-308.

FOMON SJ, JENSEN RL, OWEN GM.
1963.
Determination of body volume of infants by a method of helium displacement.
Annals of the New York Academy of Sciences, 110(Sept):80-90.

GARN SM, NOLAN P JNR.
1963.
A tank to measure body volume by water displacement (BOVOTA).
Annals of the New York Academy of Sciences, 110(Sept):91-95.

GARROW JS, STALLEY S, DIETHELM R, PITTET P, HESP R, HALLIDAY D.
1979.
A new method for measuring the body density of obese adults.
British Journal of Nutrition, 42:173-183.

GOLDMAN RF, BUSKIRK ER.
1961.
Body volume measurement by underwater weighing: description of a method.
pp.78-89 In: Brozek J, Henschel A, eds. Techniques for measuring body composition.
Washington, DC : National Academy of Sciences-National Resource Council.

GRAY PE, SEARLE CL.
1969.
Electronic principles: Physics, Models, and Circuits.
pp.65-67, New York: John Wiley and Sons.

GUNDLACH BL, NIJKRAKE HGM, HAUTVAST JGAJ.
1980.
A rapid and simplified plethysmometric method for measuring body volume.
Human Biology, 52(1):23-33.

GUNDLACH BL, VISSCHER GJW.
1986.
The plethysmometric measurement of total body volume.
Human Biology, 58(5):783-799.

KEYS A, BROZEK J.
1953.
Body fat in adult man.
Physiological Reviews, 33(3):245-325.

KODAMA AM, PACE N.
1963.
A simple decompression method for in vivo body fat estimation in small animals.
Journal of Applied Physiology, 18:1272-1276.

LIEDTKE JL.
1986.
Body composition analysis based on bioelectric impedance instrumentation.
Article published by RJL Systems, Inc.

PESLIN R, FREDBERG JJ.
1986.
Oscillation mechanics of the respiratory system.
p.164 In: Macklem PT, Mead J, eds. Handbook of physiology: The respiratory system III.
Baltimore : Williams and Wilkens.

PIERSON WR.
1963.
A photogrammetric technique for the estimation of surface area and volume.
Annals of the New York Academy of Sciences, 110(Sept):109-112.

SETO WW.
1971.
Theory and problems of acoustics (Schaum's outline series).
pp.123-125, New York : McGraw-Hill.

SHENG H-P, ADOLPH AL, SMITH EO, GARZA C.
1988.
Body volume and fat-free mass determinations by acoustic plethysmography.
Pediatric Research, 24(1):85-89.

SIRI WE.
1961.
Body composition from fluid spaces and density : Analysis of methods.
pp.223 In: Brozek J, Henschel H, eds. Techniques for measuring body composition.
Washington D.C.: National Academy of Sciences-National Research Council.

SPIEGEL MR.
1968.
Mathematical handbook of formulas and tables (Schaum's outline series).
pp.110-113, New York: McGraw-Hill.

TAYLOR A, AKSOY Y, SCOPES JW, DU MONT G, TAYLOR BA.
1985.
Development of an air displacement method for whole body volume measurement of infants.
Journal of Biomedical Engineering, 7(Jan):9-17.

WARD A, POLLOCK ML, JACKSON AS, AYRES JJ, PAPE G.
1978.
A comparison of body fat determined by underwater weighing and volume displacement.
American Journal of Physiology, 234(1):E94-E96.

WARK K.
1966.
Thermodynamics.
pp.111-116, New York: McGraw-Hill.

ZEMANSKY MW.
1951.
Heat and thermodynamics.
pp.25-27, 42-43, 57-60, 81-83, 94-96, 102-108, 112-125.
3rd ed. New York: McGraw-Hill.

APPENDICES

170PC Series

Low Pressure Gage & Differential Sensors/ Unamplified

FEATURES
- Miniature package
- Low pressure measurement

DESIGN CONSIDERATIONS

		Min.	Typ.	Max.
Excitation (VDC)	All 174PC	—	10	12
	All 176PC	—	10	16
(mA)	All 174PC	—	2.0	2.4
Response Time (msec)	All 174/176PC	—	—	1.0
Weight (grams)	All 174/176PC	—	7	—
Overpressure (see Accuracy specifications)				
Input Resistance (ohms)	All 174PC	—	4.8 K	—
	All 176PC	—	6.3 K	—
Output Resistance (ohms)	All 174PC	—	4.8 K	—
	All 176PC	—	4.0 K	—

Low Pressure Gage & Differential Sensors/ Unamplified

170PC

ENVIRONMENTAL SPECIFICATIONS

Temperature	Operating	−40° to 85°C (−40° to 185°F)
	Storage	−55° to 125°C (−67° to 257°F)
	Compensated	0° to 50°C (32° to 122°F)
Shock	MIL-STD-202, Method 213 (150 g, half sine, 11 msec)	
Vibration	MIL-STD-202, Method 204 (10 to 2000 Hz at 20 g)	
Media	P2 port	Wetted materials: polyester housing, epoxy adhesive, silicon, borosilicate glass, and silicon-to-glass bond*
	P1 port	Dry gases only

*Liquid media containing some highly ionic solutions could potentially neutralize the chip-to-glass tube bond.

Other Pressure Sensors — See Selection Guide, pages 6 & 7.

ORDER GUIDE

PRESSURE RANGE (Inches H_2O)		0-14"			0-28"		
CATALOG LISTINGS*	Basic Sensor	174PC14HG2			174PC28HG2		
Gage	Temperature Comp. Volt Excitation	176PC14HG2			176PC28HG2		
Differential	Basic Sensor	174PC14HD2			174PC28HD2		
	Temperature Comp. Volt Excitation	176PC14HD2			176PC28HD2		

ACCURACY SPECIFICATIONS at 10.0 ± 0.01 VDC Excitation, 25°C

Parameter	170PC Type	Min.	Typ.	Max.	Min.	Typ.	Max.
F.S.O. Full Scale Output (mV)	174PC	38	52.5	67	58	70	82
	176PC	33	35	37	40	42	44
Sensitivity per "H_2O (mV)	174PC	—	3.57	—	—	2.5	—
	176PC	—	2.50	—	—	1.5	—
Overpressure ("H_2O)	174/176PC	—	—	140	—	—	140
Linearity Best Fit Straight Line (%F.S.O.) Port 2 > Port 1	174PC	—	±2.0	—	—	±2.0	—
	176PC	—	—	±3.0	—	—	±3.0
Port 2 < Port 1	174PC	—	±2.0	—	—	±2.0	—
	176PC	—	—	±1.5	—	—	±1.5

			Min.	Typ.	Max.
Null Offset (mV)	All 174PC		−80	−40	0
	All 176PC		−2	0	+2
Null Shift (mV) 25° to 0°C, 25° to 50°C	All 174/176PC		—	±3.0	—
Sensitivity Shift (%F.S.O.) 25° to 0°C, 25° to 50°C	At 10 VDC:	All 174PC	—	±6.5	—
		All 176PC*	—	—	±4.0
		All 176PC*	—	—	±3.5
	At 2 mA:	All 174PC	—	±5.5	—
Repeatability & Hysteresis (%F.S.O.)	All 174/176PC		—	±0.25	—
Stability over One Year (%F.S.O.)	All 174/176PC		—	±0.5	—

Key: b = 0-14" H_2O only
h = 0-28" H_2O only

Catalog listings are shown with terminal style 2. To order style 1 (or 3), substitute the number 1 (or 3) for the 2 at the end of the listing

174PC
No calibration
No temperature compensation
Lower price

176PC
Calibrated Null and F.S.O.
Temperature compensated for F.S.O. over 0 to 50°C
Provides interchangeability

*Bold listings—Normally in stock.
Light listings—Check MICRO SWITCH distributor or Sales Office for availability.

ELECTRICAL CONNECTIONS

Voltage Excitation
174/176PC

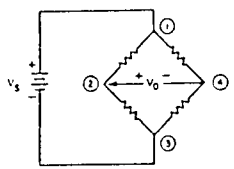

Current Excitation
174PC

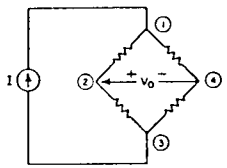

NOTES
1. Circled numbers refer to sensor termination.
2. V_O changes with pressure difference.
3. $V_O = V_2 - V_4$ (referenced to pin 3).
4. Current excitation provides reduced sensitivity variation with temperature.

INTERNAL CIRCUITRY

176PC

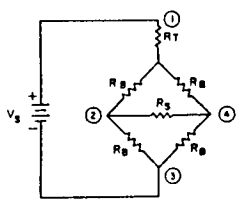

174PC

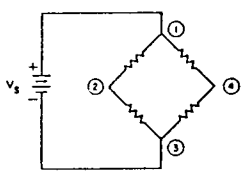

NOTES
1. Circled numbers refer to sensor termination.
2. $V_O = V_2 - V_4$ (referenced to pin 3).
3. R_S = Strain gage resistors (~ 4.8 kΩ).
4. R_T = Sensitivity temperature compensation resistor.
5. R_S = Sensitivity calibration resistor.

When a positive pressure is applied to port P2, the differential voltage $V_2 - V_4$ (voltage at pin 2, with respect to ground, increases and voltage at pin 4 decreases) increases linearly with respect to the input pressure. When a vacuum pressure is pulled at port P2 (or positive pressure applied to port P1) the voltage $V_2 - V_4$ decreases linearly with respect to the input pressure.

SENSITIVITY SHIFT

The diagram at right illustrates how sensitivity shift relates to temperature. Note that the maximum shift occurs at temperature extremes. Therefore, if a sensor is not exposed to the entire temperature range, the maximum sensitivity shift will actually be less than the value specified.

SENSITIVITY SHIFT (% F.S.O.)

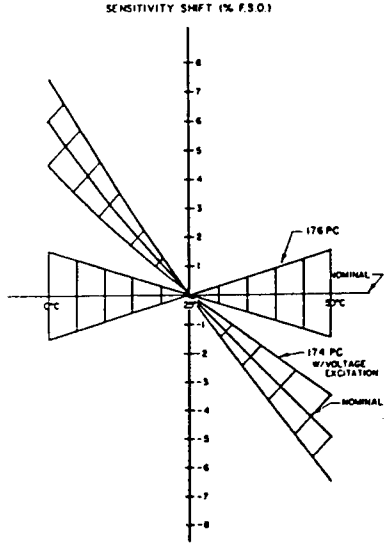

A2

MOUNTING DIMENSIONS (For reference only)

Gage Types

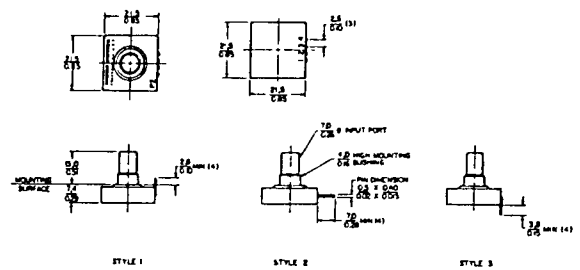

Terminals
1 – Vs (+)
2 – Output A
3 – Ground (–)
4 – Output B

Differential Types

Mounting Hardware

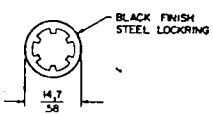

Catalog listings are shown with terminal style 1. To order style 2 (or 3), substitute the number 2 (or 3) for the 1 at the end of the listing.

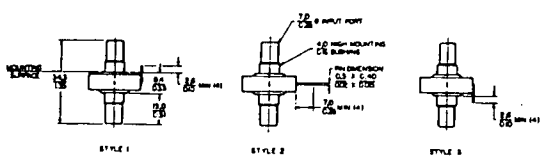

170PC CONSTRUCTION

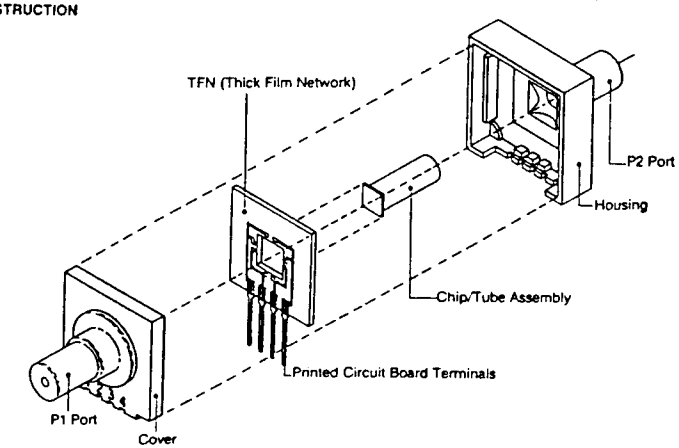

SenSym

LX05XXA and LX06XX Series Low and Mid-Pressure Range Monolithic Pressure Transducers

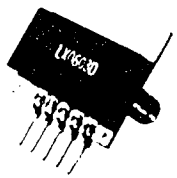

General Description

The monolithic pressure transducers are piezoresistive integrated circuits which provide an output voltage proportional to applied pressure. The devices are provided in compact packages with pressure ports, suitable for PC board mounting and attachment of flexible tubing.

The LX05XXA is an absolute pressure transducer with a single pressure inlet tube axially aligned with its TO-5 package, suitable for use with non-ionic working fluids.

The LX06XXGB is a gage transducer with a single tube and an ambient inlet. It is well suited for use with package-compatible working fluids, including water.

The LX06XXD is a differential pressure transducer with two pressure ports, suitable for use with non-ionic working fluids in either pressure port, and package-compatible working fluids in the positive pressure port.

See Application Guide — Media Compatibility

Advantages of Monolithic

The monolithic transducers include only the basic monolithic pressure IC chip used in Sensym's signal-conditioned pressure transducer products. This greatly reduces unit cost and allows the electronic designer greater freedom in implementing transducer circuits. The monolithic transducer is temperature compensated with respect to sensitivity and features low offset temperature coefficient. High sensitivity and low noise allow easy amplification. These devices are especially useful in applications requiring battery power, circuit flexibility, or compatibility with microprocessors.

Features

- Low cost
- Interface circuit flexibility
- Temperature compensation of span
- Compact, PC board compatible
- Low noise
- High natural frequency
- Low volumetric displacement
- Separate temperature-sensitive output

Applications

- Automated equipment
- Residential, commercial and industrial controls
- Medical diagnostics
- Automotive diagnostics and controls
- Machine tool controls
- Barometry

Schematic Diagram

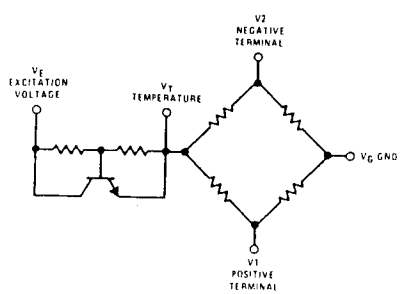

Electrical Connections

Symbol	LX05XX	LX06XX
V_E	3	5
V_T	7	1
V1	6	3
V2	5	4
V_G	8	2

Pressure Transducer Characteristics

Maximum Ratings

Excitation Voltage, V_E	12V
Operating Temperature Range	−40°C to +105°C
Pressure Range	
LX0503A	100psia
LX0603D	±45psid
LX0603GB	45psig
Common Mode Line Pressure, LX0603D	200psig
Bridge Voltage, V_T	≤ V_E
Lead Temperature (Soldering, 10 seconds)	200°C

Reference Conditions (Note 1)

Excitation Voltage, V_E	7.5V
Reference Temperature	25°C
Reference Temperature Range	0°C to 50°C
Offset Reference Pressure (Note 5)	
LX0503A	0psia
LX0603D	0psid
LX0603GB	0psig
Common Mode Line Pressure, LX0603D	0psig

Performance Characteristics

Device Type	Operating Pressure Range	Guaranteed Specifications			Typical Specifications						
		Offset Calibration	Linearity, Hysteresis and Repeatability (Note 2)		Offset Repeatability (Note 3)		Offset Stability (Note 4)		Span Sensitivity Calibration	Span Stability (Note 4)	
		mV	±%FS	±psi	±%FS	±psi	±%FS	±psi	mV/psi	±%FS	±psi
LX0503A	0 to 30 psia	0 ± 100	1.00	0.3	0.4	0.12	1.7	0.5	2 to 8	0.3	0.09
LX0603D	0 to ±30 psid	0 ± 100	1.00	0.6	0.4	0.24	0.8	0.5	2 to 8	0.3	0.18
LX0603GB	0 to +30 psig	0 ± 100	1.00	0.45	0.4	0.18	1.1	0.5	2 to 8	0.3	0.14

Device Type	Operating Pressure Range	Typical Characteristics					
		Offset Shift w/Temperature (0°C to 50°C) (Note 6)	Sensitivity w/Temperature (0°C to 50°C) (Note 7)	Bias Current	Bridge Resistance	Diaphragm Natural Frequency	Compensation Circuit Temperature Coefficient (Note 8)
		±mV	±%FS	mA	kΩ	kHz	mV/°C
LX0503A	0 to 30 psia	2	0.5	2.0	1.8	50	−10.0
LX0603D	0 to ±30 psid	2	0.5	2.0	1.8	50	−8.0
LX0603GB	0 to +30 psig	2	0.5	2.0	1.8	50	−8.0

Specification Notes:

Note 1: Conditions at which "Performance Characteristics" are specified.

Note 2: Linearity — the maximum deviation of measured output, at constant temperature (25°C), from "best straight line" through three points (offset pressure, full scale pressure, one-half full scale pressure).

$$\%\ FS\ error = \frac{V_{\frac{1}{2}\ full\ scale} - \left[\left(\frac{(V_{full\ scale} - V_{offset})}{full\ scale\ pressure}\right) \times \left(\frac{1}{2}\ full\ scale\ pressure\right) + V_{offset}\right]}{2} \times 100\%$$

(V = measured value for each device)

Note 3: Offset Repeatability — the transducer's ability to reproduce offset voltage at constant temperature (25°C) when cycled through its full operating pressure range.

Note 4: Stability — the transducer's ability to reproduce the output voltage corresponding to a specific pressure and temperature in a period of one year during which maximum ratings are not exceeded.

Note 5: Offset Reference Pressure — the lowest pressure in the operating pressure range.

Note 6: Temperature error is measured into an infinite impedance without offset adjusted.

Note 7: Voltage applied at V_E, with no offset nor sensitivity adjust.

Note 8: Compensation Circuit Temperature Coefficient $\Delta V_{ET}/\Delta T$ — the change in voltage across the compensation circuit, $V_{ET} = V_E - V_T$, as the temperature changes within the permitted operating range.

Pressure Transducer Characteristics

Maximum Ratings

Excitation Voltage, V_E	12V
Operating Temperature Range	−40°C to +105°C
Pressure Range	
LX0520A	200psia
LX0620D	±150psid
LX0620GB	150psig
Common Mode Line Pressure, LX0620D	200psig
Bridge Voltage, V_T	≤ V_E
Lead Temperature (Soldering, 10 seconds)	200°C

Reference Conditions (Note 1)

Excitation Voltage, V_E	7.5V
Reference Temperature	25°C
Reference Temperature Range	0°C to 50°C
Offset Reference Pressure (Note 5)	
LX0520A	0psia
LX0620D	0psid
LX0620GB	0psig
Common Mode Line Pressure, LX0620D	0psig

Performance Characteristics

Device Type	Operating Pressure Range	Guaranteed Specifications			Typical Specifications						
		Offset Calibration	Linearity, Hysteresis and Repeatability (Note 2)		Offset Repeatability (Note 3)		Offset Stability (Note 4)		Span Sensitivity Calibration	Span Stability (Note 4)	
		mV	±%FS	±psi	±%FS	±psi	±%FS	±psi	mV/psi	±%FS	±psi
LX0520A	0 to 30 psia	0 ± 50	1.00	1.00	0.4	0.40	1.2	1.2	0.2 to 0.8	0.3	0.30
LX0620D	0 to ±100 psid	0 ± 80	1.00	2.00	0.4	0.80	0.6	1.2	0.2 to 0.8	0.3	0.60
LX0620GB	0 to +100 psig	0 ± 50	1.00	1.15	0.4	0.46	1.0	1.2	0.2 to 0.8	0.3	0.35

Device Type	Operating Pressure Range	Typical Characteristics					
		Offset Shift w/Temperature (0°C to 50°C) (Note 6)	Sensitivity Shift w/Temperature (0°C to 50°C) (Note 7)	Bias Current	Bridge Resistance	Diaphragm Natural Frequency	Compensation Circuit Temperature Coefficient (Note 8)
		±mV	±%FS	mA	kΩ	kHz	mV/°C
LX0520A	0 to 100 psia	0.67	0.5	2.0	1.8	100	−10.0
LX0620D	0 to ±100 psid	0.67	0.5	2.0	1.8	100	−8.0
LX0620GB	0 to +100 psig	0.67	0.5	2.0	1.8	100	−8.0

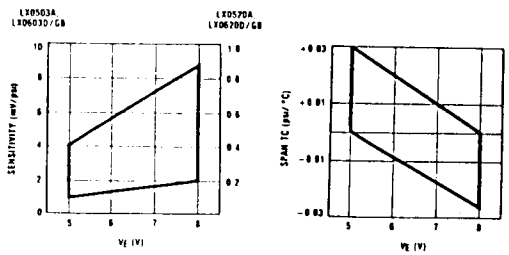

Figure 1. Typical Ranges of Sensitivity and Span TC vs. Applied Voltage V_E for LX05XXA and LX06XXD, GB Pressure Transducers

Typical Physical Dimensions Inches (millimeters)

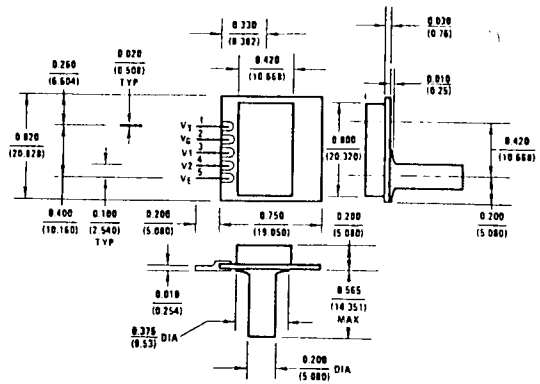

PX6B
Package for LX06XXGB Series Pressure Transducers
Weight: 5 grams

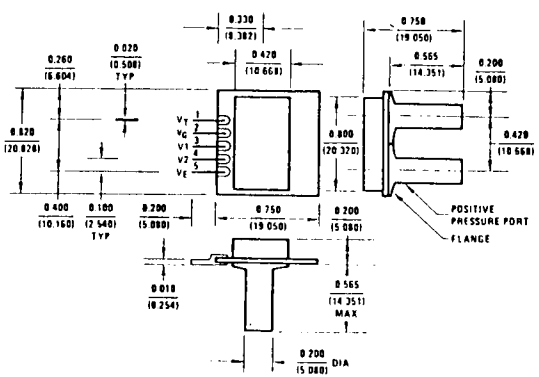

PX6D
Package for LX06XXD Series Pressure Transducers
Weight: 5 grams

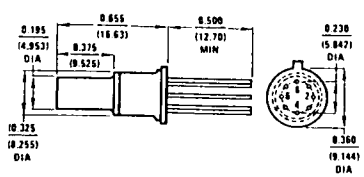

PX5A
Package for LX05XXA Series Absolute Pressure Transducers
Weight: 1.5 grams

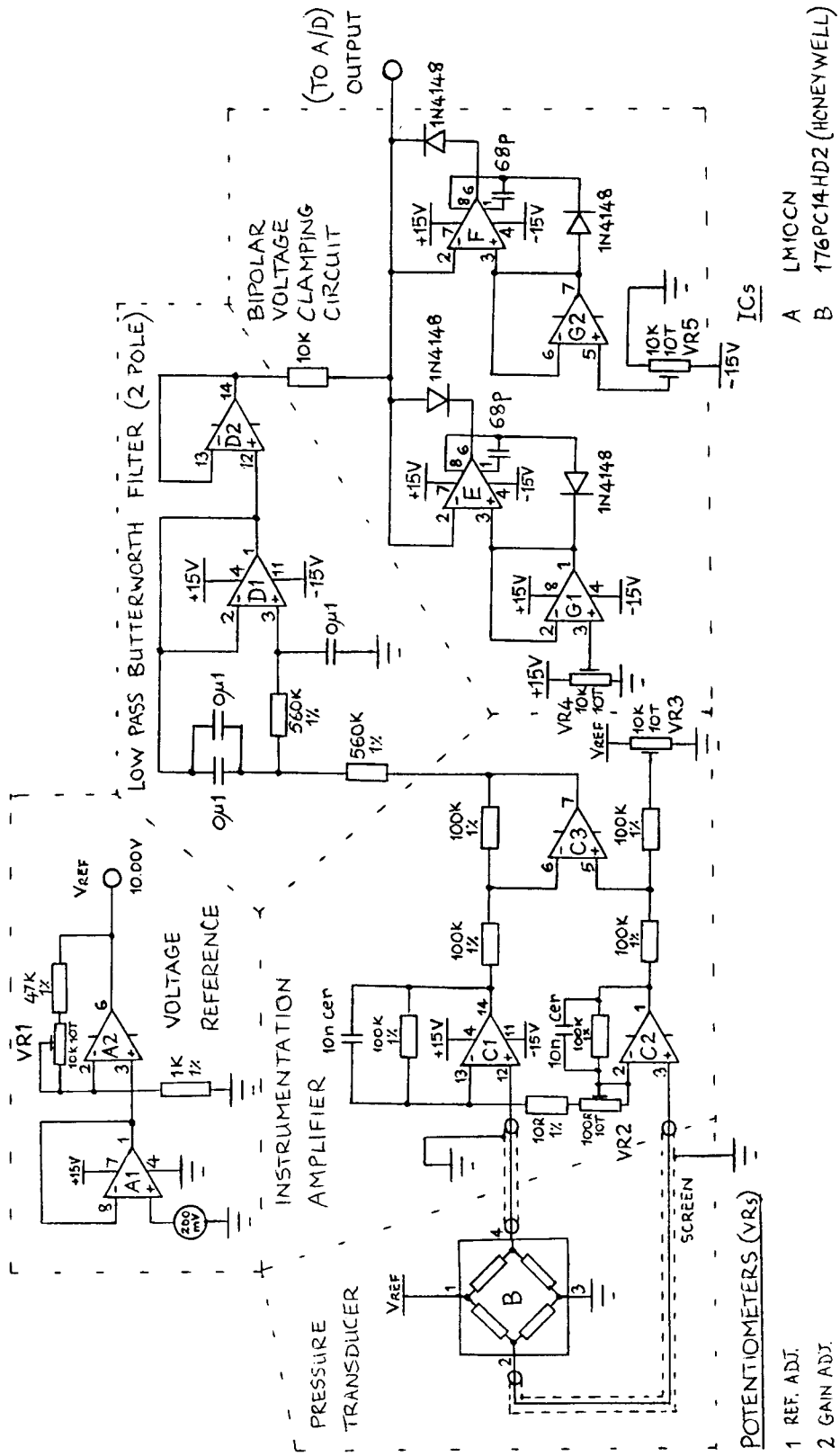
DIFFERENTIAL PRESSURE TRANSDUCER CIRCUIT
PRESSURE TRANSDUCER
INSTRUMENTATION AMPLIFIER
VOLTAGE REFERENCE
LOW PASS BUTTERWORTH FILTER (2 POLE)
BIPOLAR VOLTAGE CLAMPING CIRCUIT
(TO A/D) OUTPUT
SCREEN
POTENTIOMETERS (VR's)
1 REF. ADJ.
2 GAIN ADJ.
3 OFFSET ADJ.
4 POS. LIMIT
5 NEG. LIMIT
ICs
A LM10CN
B 176PC14HD2 (HONEYWELL)
C LM324N
D LF444
E/F LM301
G LM358

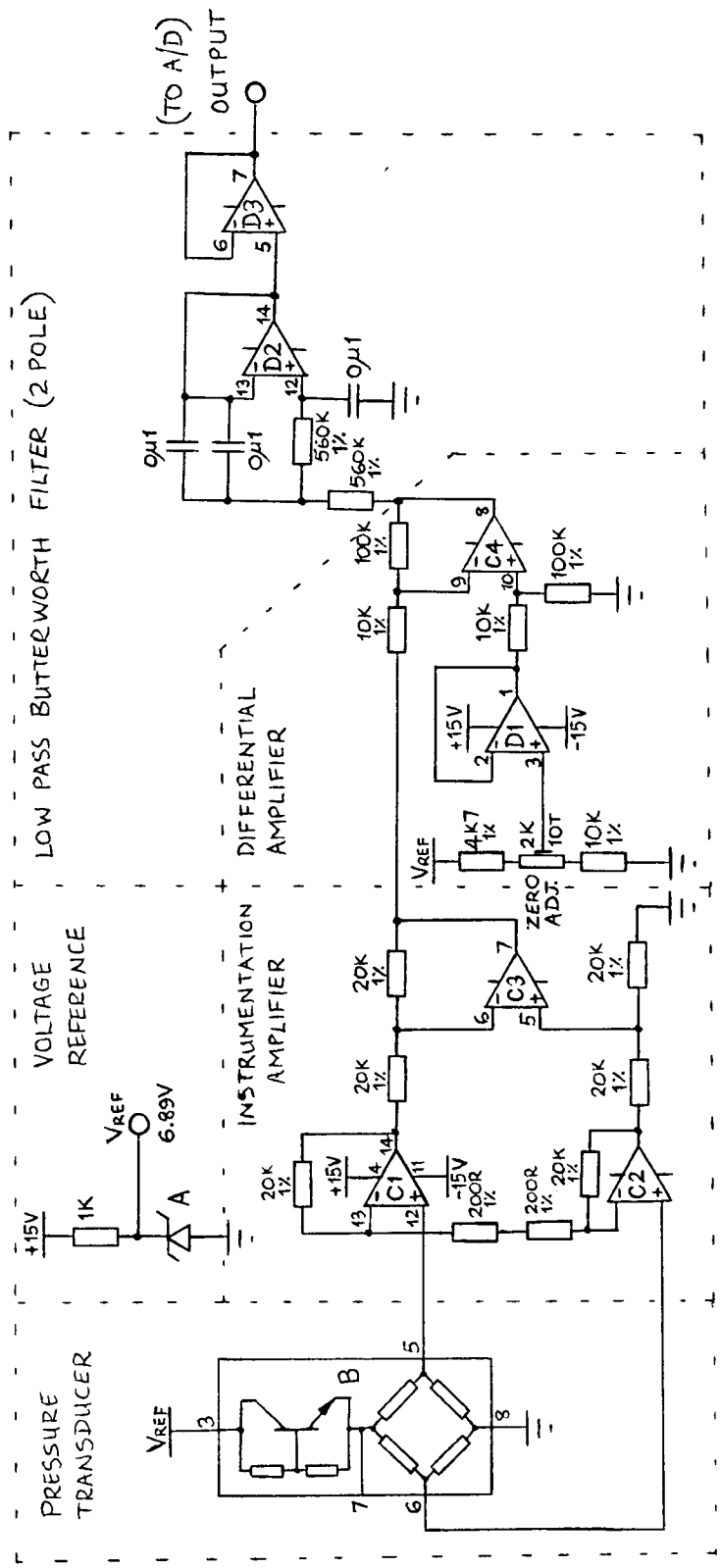

ICs
A LM329A/B
B LX0503A(SENSYM)
C LM324N
D LF444

ABSOLUTE PRESSURE TRANSDUCER CIRCUIT

APPENDIX E : ANALYSIS OF ALGORITHM ERROR

From figure E.1 it is evident that the algorithm extracted values are underestimated, the degree of which is dependent on the slope. The rise over the period of a half-wave is assumed to be linear (compared to the typical rise time constant, which is of the order of ten times or more). The pressure wave may be presented in the following general form:

$$P(t) = a\sin\omega t + bt + c \qquad (1)$$

the first term representing the sine wave, the second term the slope, and the last term the offset. More specifically, the expression may be written as:

$$P(t) = \frac{\Delta p}{2}\sin\frac{2\pi}{\tau_c}t + \frac{\delta p}{\tau_{\frac{1}{2}c}}t + P_{OFFSET} \qquad (2)$$

where Δp is the true "delta", τ_c is the time taken to complete a full cycle or wave, $\tau_{\frac{1}{2}c}$ is the time taken to complete a half cycle or wave, and δp is the linear rise in pressure during a half wave. The algorithm extracts the "deltas" at the local maxima and minima (where the derivative of the pressure wave is zero). If the derivative of the above expression is set to zero, the first maximum value is:

$$P_{MAX1} = \frac{\Delta p}{2}\sin[\arccos(-\frac{2\delta p}{\pi\Delta p})] + \frac{\delta p}{\pi}\arccos(-\frac{2\delta p}{\pi\Delta p}) \qquad (3)$$

which differs from the true "delta" by a factor of:

$$\sin[\arccos(-\frac{2\delta p}{\pi\Delta p})] = \cos[\arcsin(\frac{2\delta p}{\pi\Delta p})] \qquad (4)$$

as seen in the first term. The true "delta" is therefore:

$$\Delta p = \frac{\Delta p'}{\cos[\arcsin(\frac{2\delta p}{\pi\Delta p})]} \doteq \frac{\Delta p'}{\cos[\arcsin(\frac{2\delta p}{\pi\Delta p'})]} \qquad (5)$$

where Δp represents the true "delta", and $\Delta p'$ represents the algorithm extracted "delta".

The right hand side of this final expression is reliable if the ratio $\delta p/\Delta p'$ is kept less than say 0.2. A typical value for the ratio $\delta p/\Delta p'$ is 0.02 and the maximum encountered value was 0.04. Thus the typical correction factor required is 1.00008 (error of 0.008 %), with a worst case of 1.00032 (error of 0.032 %), which resembles a quadratic relationship. By performing a sensitivity analysis on the body volume expression from chapter 3 (see appendix I), with respect to Δp , a sensitivity of 0.901 is found. This means that an error of volume of 0.00029 l (for a 70 l man), which is practically negligible, exists.

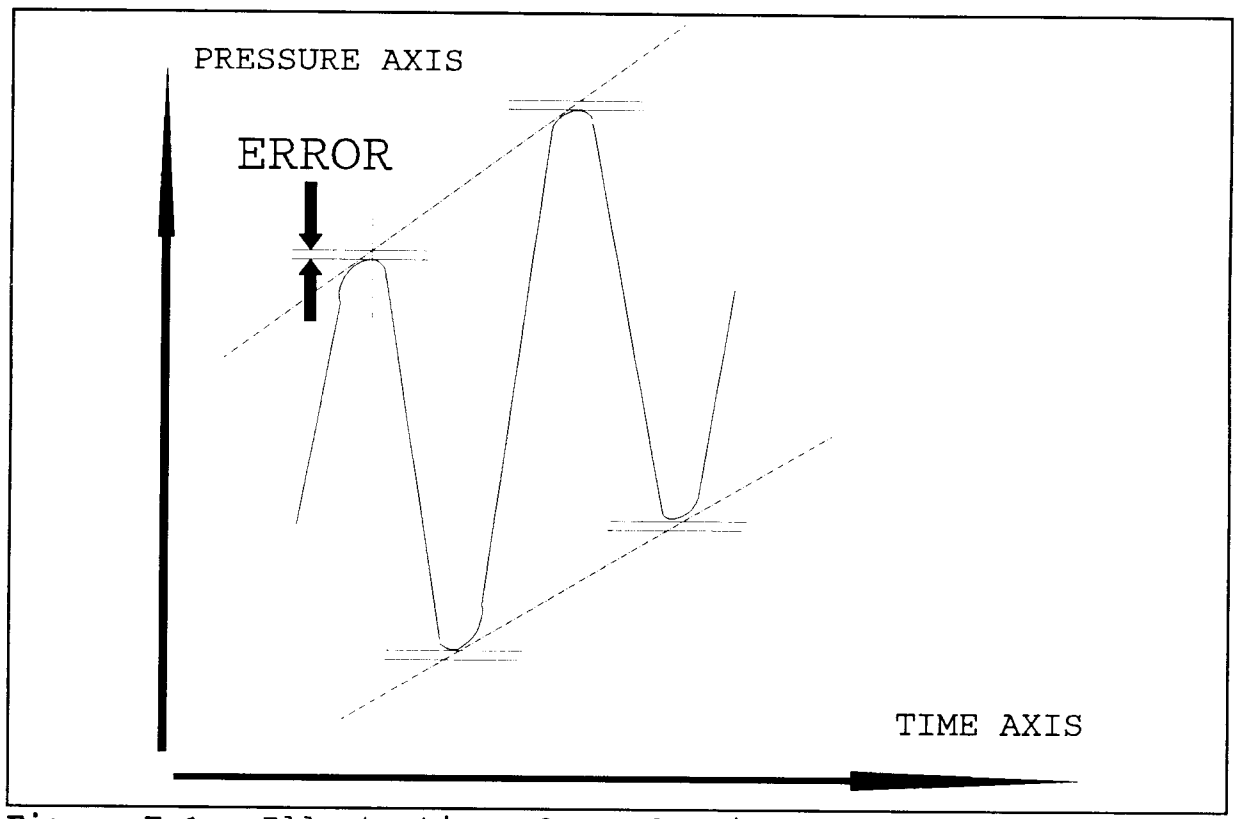

Figure E.1 : Illustration of an algorithm error.

APPENDIX F : UNDERWATER WEIGHING DATA

Underwater weighing is considered the most accurate indirect means of measuring body fat and serves as the gold standard for other indirect methods. It involves Archimedes' principle of water displacement which states that a body immersed in water is buoyed up with a force equal to the weight of the water displaced. The body volume is then measured by determining the weight loss by completely submerging it in water. The subject is asked to exhale completely when submerging himself (herself), and to lie as still as possible for as long as his/her "breath" lasts. To ensure reasonable accuracy, corrections are made by taking the residual lung volume and the water temperature (density) into consideration. These parameters must therefore also be measured. From the literature (Goldman and Buskirk, 1961) an expression is found that relates body volume to body weight (land), underwater weight, water density and residual lung volume.

$$BODY\ VOLUME = \frac{BODY\ WGT - UNDERWATER\ WGT}{WATER\ DENSITY} - RES.\ LUNG\ VOLUME$$

where *WGT* and *RES.* are abbreviations for weight and residual, respectively.

Calculation of the percent body fat is facilitated by using Siri's (1961) expression relating % body fat, mass and volume (see Introduction).

The employment of this method however, was carried out under difficult circumstances. Within the environs of Cape Town no specific underwater weighing setup existed around the time of the testing. Firstly a scale had to be acquired. A suspension scale was loaned from S.A. Scale (Cape Town, South Africa). It was a new, large, round-faced, mechanical Salter weighing scale (25 kg with 50 g gradations). The Cape Town winter called for the use of an indoor pool. This pool had to be equipped with an overhanging structure from which the subject to be weighed is to be suspended. The staff of the rehabilitation centre

(biokinetics dept., 2 Military Hospital, Wynberg, Cape Town) offered the use of their facilities and assisted with enthusiasm. However, the water was unheated with water temperatures in the region of 18 to 20 ^{0}C. This caused the subjects to shiver, making it difficult to read the underwater weight accurately due to scale fluctuations.

Each subject (in a swimming costume) was asked to wet himself (herself) and to "glide" onto a submerged, suspended stretcher, with his/her head above the water's surface for breathing. The subject was then instructed to hyperventilate a little whereafter he/she exhaled maximally, then submerged entirely while clinging to the stretcher. While submerging he/she would then attempt to remove as much bubbles as possible. After a few seconds the entire suspended unit (subject and stretcher) would stabilize, after which a reasonably stable underwater weight reading would be taken. After about 10 to 15 seconds the subject would surface. This procedure was repeated a few more times until readings were repeatable. The "heaviest" stable reading would generally be taken as this suggests that the subject was more bubble-free and was closer to the true residual lung volume. The subjects were untrained as it was unreasonable to train them in such cold water. It was important not to stir or agitate the water as this would cause additional fluctuations, making it even more difficult to read the scale.

Hereafter the lung volumes were measured. Clinical technologists at the Groote Schuur Hospital in Observatory, Cape Town, performed lung function tests on the subjects, making use of the Jaeger Body Plethysmograph. Specifically, the static lung volumes (including the residual volumes) were measured. Then one of the subjects were asked to have these measurements repeated. However, consecutive readings on the same subject proved unreliable, and these data were rejected. The helium dilution technique was then employed at the Red Cross Children's Memorial Hospital in Rondebosch, Cape Town. A P.K. Morgan Helium Dilution system, which was calibrated very recently, was used.

All relevant data as well as body volumes and percent body fat appear in table F.I.

Table F.I : Underwater weighing estimates of body volume and percent body fat.

SUBJ #	BW (kg)	UWW (kg)	WT (°C)	WD (g/cc)	RV (l)	BV (l)	%BF (%)
1	71.5	2.75	18.8	0.99847	1.46	67.40	16.6
2	56.8	0.70	18.8	"	1.27	54.92	28.6
3	59.4	0.90	18.8	"	0.66	57.93	32.7
4	67.5	1.45	18.8	"	1.15*	65.00*	26.7*
5	74.2	3.15	20.4	0.99815	2.17	69.11	10.4
6	72.4	3.65	20.4	"	0.35	68.53	18.5
7	62.8	2.90	20.4	"	1.07	58.94	14.6
8	83.5	3.90	20.4	"	1.14	78.61	16.0

* At the time of the lung function tests this subject was not available (airway infection). The predicted RV value was used (according to the Jaeger Masterlab Plethysmograph).

Key to the above table:

SUBJ	subject
BW	body weight (on land)
UWW	underwater weight
WT	water temperature
WD	water density
RV	residual lung volume (corrected to B.T.P.S.)
BV	body volume
%BF	percent body fat

APPENDIX G : BIOIMPEDANCE ANALYSIS DATA

Two bioimpedance methods were employed. The RJL bioimpedance analyzer (RJL) of RJL Systems Inc., U.S.A., and the Bodystat 500 impedance analyzer (BS) of Bodystat CC, Cape Town, South Africa, was used. The former instrument measures the total body resistance as well as reactance at a frequency of 50 kHz, while the latter only measures the impedance at a similar frequency. The measured values give an indication of the total body water, from which the lean body mass is derived. The fat mass is acquired by subtracting the lean mass from the total body mass. After inserting the readings as well as complementary data like height, body mass, gender, and age into a computer program, the total body water, lean body mass and fat mass is provided.

Each subject was asked to relax while lying down on a bed (the surface of which is non-conductive) on his/her back with the limbs straightened, at about 20 degrees from the median. After shaving specific sites (about 1 cm proximal of an imaginative line intersecting the meta- carpo/tarso -phalangeal joints, and the centre of an imaginative line intersecting the malleoli) on the dorsal side of the subject's right hand and right foot, disposable, conductive gel-coated electrodes were secured to these sites, and connected to the instrument. To ensure reproducibility these measurements were repeated until consecutive readings were similar to within 1 ohm.

By using Siri's (1961) expression relating % body fat, mass and volume (see Introduction) we arrive at the volumes as presented in the following table:

Table G.I : Bioimpedance analysis estimates of percent body fat and body volume.

SUB-JECT #	BODY MASS (kg)	AGE (yr)	GEN-DER (M/F)	HGT (cm)	REACT RJL (ohm)	RESIST RJL (ohm)	RESIST BS (ohm)	%BODYFAT RJL (%)	%BODYFAT BS (%)	BODYVOL RJL (l)	BODYVOL BS (l)
1	71.5	17	M	176	68	526	533	20	13.4	67.9	66.9
2	56.8	29	F	163	59	601	599	26	23.6	54.6	54.3
3	59.4	18	F	170	68	733	760	27	25.7	57.2	57.1
4	67.5	17	F	166	70	626	639	33	29.0	65.9	65.3
5	74.2	31	M	184	48	448	448	11	8.7	69.1	68.8
6	72.4	24	M	173	56	420	420	13	9.5	67.7	67.2
7	62.8	23	M	177	56	576	580	18	12.7	59.4	58.7
8	83.5	28	M	187	49	443	450	14	12.0	78.3	77.9

Key to table:

HGT	Subject height;
REACT	Reactance at 50 kHz;
RESIST	Resistance at 50 kHz;
BODYVOL	Body volume;
RJL	RJL instrument estimate;
BS	Bodystat instrument estimate.

APPENDIX H : SKINFOLD DATA

The 4-fold Durnin and Rahaman method was employed. The person who performed these measurements was well trained in the technique and was in good practice at the time. It is well known that the accuracy of this method relies on these factors.

Each subject was asked to stand upright and relax. The sites (right tricep, right bicep, right subscapula, and right supra-ileum) were marked by pen so as to ensure reproducibility. The skinfolds of the areas were measured in similar order. Then these measurements were repeated twice in succession. A third party who ensured that the operator could not see previous data, collected the data. For each site a mean was calculated. The four means were simply added and a corresponding fat percentage value was read off from a wall chart (separate columns for males and females).

An excerpt of the raw data appears in table H.I (all values in mm):

Table H.I : Complete skinfold data of one subject.

SUBJECT #7	trial #1	trial #2	trial #3	MEAN
tricep	3.0	2.8	2.8	2.9
bicep	6.6	6.6	6.4	6.5
subscapula	8.0	8.0	7.8	7.9
supra-ileum	4.6	4.6	4.9	4.7

			TOTAL =	22.0

Therefore, from wall chart, % fat = 10 (rounded).

By using Siri's (1961) expression relating % body fat, mass and volume (see Introduction) the volumes, as presented in table H.II, were calculated.

Table H.II : Skinfold estimates of percent body fat and body volume.

SUBJECT #	% BODY FAT (%BF)	BODY MASS (kg)	BODY VOLUME (l)
1	16	71.5	67.3
2	23	56.8	54.3
3	27	59.4	57.2
4	30	67.5	65.5
5	8	74.2	68.7
6	12	72.4	67.6
7	10	62.8	58.4
8	11	83.5	77.8

APPENDIX I : SENSITIVITY ANALYSIS

The differential of $f(x,y,z)$ is (Spiegel, 1968):

$$df = \frac{\partial f}{\partial x}dx + \frac{\partial f}{\partial y}dy + \frac{\partial f}{\partial z}dz \qquad (1)$$

The previously derived expression, relating the displaced volume V_B to the chamber volume V_C , the stroke volume ΔV , the chamber pressure P_C , the pressure delta Δp , and the specific heat ratio k, follows (see chapter 3):

$$V_B \approx V_C - \frac{(k+1)\Delta V}{2} - \frac{kP_C\Delta V}{\Delta p} \qquad (2)$$

By differentiating this expression, the sensitivity of V_B, in relation to its parameters, follows:

$$dV_B = \sum_1^n \frac{\partial V_B}{\partial X_i}dX_i \qquad (3)$$
$$(X_i = V_C, \Delta V, P_C, \Delta p, k)$$

The sensitivity of V_B with respect to k is thus:

$$dV_B(k) = \frac{\partial V_B}{\partial k}dk \qquad (4)$$

from which:

$$\frac{\partial V_B}{\partial k} \approx -2\ \Delta V\frac{P_C}{\Delta p} \qquad (5)$$

For a typical case of a 70 l man at S.T.P. (standard temperature and pressure), with a stroke volume of 0.8 l, the pressure variation will be about 350 Pa, which yields a sensitivity of the end product, or volume, with respect to k , as:

$$dV_B(k) \approx -460\,dk \qquad (6)$$

A variation, or change in k will thus be "amplified" negatively by a factor of 460, which means that the end-product of the device, namely volume, is very sensitive to k.

A similar sensitivity analysis of V_B with respect to pressure variation Δp for the above case yields a sensitivity of 0.901.